



# Comparative assessment of slope stability along road-cuts through rock slope classification systems in Kullu Himalayas, Himachal Pradesh, India

Rahul Khanna<sup>1,2</sup> · R. K. Dubey<sup>1</sup>

Received: 18 May 2020 / Accepted: 22 October 2020 / Published online: 4 November 2020  
© Springer-Verlag GmbH Germany, part of Springer Nature 2020

## Abstract

Evaluation of stability of artificial slopes created due to road construction in the mountainous terrain is very important but often a neglected aspect. The safe execution of road-cut slopes depends upon the level of understanding achieved in defining the engineering behaviour of rock masses with respect to its deformation and mechanical attributes. Understanding the realistic response of the rock mass to excavation of rock strata requires proper analysis related to influence of structural elements on their continuous characterization for facilitating safe and economical development of cut slopes along the road sections. In this paper structurally and non-structurally controlled rock slope classification systems are implemented to undertake comprehensive evaluation of stability of road-cut slopes. The work carried out involves collection of various inputs in form of rock mass and discontinuity characteristics from ten cut slopes along a road section in Kullu area, Himachal Pradesh, India. Rock samples were collected from site and laboratory testing has been undertaken to determine the intact rocks strength. Beside these, the kinematic analysis was performed to illustrate the geometrical relationship between various joint sets and the slope face so as to determine their failure mechanism. Several rock mass classification systems developed for rock slope stability assessment are evaluated for known slope conditions. The stability assessment for all identified cut slopes is compared using slope mass rating (SMR), Q-slope and slope stability rating (SSR) methods. Design charts proposed for various factor of safety values have been utilized to evaluate the stability of studied road-cut slopes. Finally, a slope wise comparison is made between the stable angles predicted by SSR with those recommended by Q-slope method.

**Keywords** Slope stability · Rock mass classification · Slope mass rating (SMR) · Slope stability rating (SSR) · Q-slope · Kinematic analysis · Kullu Himalayas (India)

## Introduction

Likewise other mountainous terrains of the world, Himalayan region also constitute a complex network of roads which form a major mode of communication in the region. In India, with major infrastructure boom coming up during last few years, road network is rapidly growing in this highly vulnerable and

undulatory terrain. Road construction in mountainous regions requiring excavation for new alignment and widening purpose decline the stability of the slopes (Janardhana et al., 2018). With this fast growing network, problems of slope stability and slope failure along the newly constructed road-cuts are subject of major concern in the Himalayas. Rock slopes located in mountainous terrain are prone to instability problems mainly due to variation in rock mass conditions and combination of external forces induced by environment such as rainfall and seismic events which act as triggering factors. Several incidences of major and minor landslides are reported in hilly terrain during monsoon season due to heavy rainfall. Such incidence continues even up to post monsoon month when severity of rainfall decreases. Therefore, the stability of rock slopes is considered vital to public protection in highways passing through rock cuts, as well as to people and equipment safety in open-pit mines of mountainous regions (Basahel and

---

✉ R. K. Dubey  
rkdubey1085@hotmail.com

Rahul Khanna  
rahulgeo05@gmail.com

<sup>1</sup> Indian Institute of Technology (Indian School of Mines),  
Dhanbad, India

<sup>2</sup> NHPC, Faridabad, India

Mitri, 2017). Very often surface excavation for widening of road and construction projects are executed without proper evaluation of geological, geotechnical and external triggering factors influencing the stability of slopes. This shortcoming is later on manifested in form of slope failure and landslides.

Understanding the engineering behaviour of rock masses and their response to surface excavation is an important aspect of slope stability analysis. Several techniques are being utilized for assessment of slope stability following either of numerical modelling, analytical, observational or empirical approaches. Numerical modelling approach is used to understand complex slope geometries and failure mechanisms. It provides insight into the effect of stress distribution in the slope and displacement on its behaviour (Wyllie and Mah, 2004). Analytical approach includes boundary element method, finite difference method or finite element method which defines detailed rock properties and involves complex computations. Empirical approach is based on relating the experience gained from other sites to condition anticipated at the present site. The rock mass classification, in specific, the slope mass rating (SMR), continues to be the favoured initial method in small-scale evaluation of rock slope stability (Salmanfarsi, et al., 2020). SMR method (Romana, 1985; Romana, 1993) is one of the most widely used and accredited empirical technique for the study of slope stability. This method is based on the rock mass rating (RMR) technique proposed under geomechanical classification of rock mass (Bieniawski, 1979, Bieniawski, 1989). SMR utilizes five basic rock mass parameters gathered in the field from the rock slopes viz., strength, rock quality designation (RQD), spacing of discontinuity, condition of discontinuity and ground water condition. SMR includes basic RMR along with four adjustment factors which depends on the existing relationship between joints present in the rock mass and the rock slope and method of slope excavation respectively. The adjustment factors computed using Romana's approach are more of decision based and discrete in nature. SMR index is very effective for the assessment of the stability of rock slopes. Later, it was slightly modified (Anbalagan et al., 1992) for including wedge failure along with plane and toppling failures. Another approach for the estimation of above adjustment factors has been proposed using continuous functions (Tomás et al., 2007). The slope mass rating calculated using Tomas approach is termed as continuous slope mass rating (CSMR). This method allows discrimination between the rock slopes with similar quality and eliminates ambiguity resulting from their calculus. The value assigned to each correction factor is unique and thus SMR estimated by continuous approach is more accurate and representative of the slope. Another classification system known as Chinese slope mass rating was proposed by Chen, where two coefficients, viz., slope height factor ( $\zeta$ ) and the discontinuity factor ( $\lambda$ ) were added to Romana's SMR. The Chinese slope mass rating is applicable

for slope height more than 80 m and if the slope height is below or equal to 80 m, this rating system is applied without the factor of slope height (Chen, 1995).

A remarkable advancement occurred through development of an engineering geology based classification known as geological strength index (GSI) with a profound purpose to overcome the difficulties faced while classifying weak rock masses (Hoek and Brown, 1997, 2019). It is independent parameter and its value relies on visual examination of rock slope surface (Dixit et al., 2017). Thus, it is observation based and simple to be applied in the field. It allows the influence of variables, which make up a rock mass, to be assessed for better understanding of rock mass behaviour (Marinos 2017; Marinos and Carter, 2018; Marinos et al., 2005). In this system, a range of GSI values for a given rock mass exposed on a slope can be picked through a chart which has on its one axis, rock classes based on their blockiness and on the other axis, range of values based on condition of the joint is given. Since its inception several modifications has been made in GSI index. One of the most significant contributions has been made by providing a quantitative basis for estimating precise value of this index (Sonmez and Ulusay, 2002). In this modified chart, a unique value of GSI is picked by defining rock classes based on structural rating (SR) on one axis and surface condition rating (SCR) on the other. SR is based on the volumetric joint count ( $J_v$ ) and it represents five rock mass categories ranging between 5 and 100. The relationship between SR and  $J_v$  is given in the chart. SCR is based on roughness, weathering and joint filling and its value ranges from 0 to 18. Another attempt concern to GSI was made by Cai et al. (2004) and Cai et al. (2007) in which two factors viz., block volume ( $V_b$ ) and a joint condition factor ( $J_v$ ) were proposed to quantify the rock characterization through this system. Further, the two vertical and horizontal scales of the original GSI charts (Hoek and Marinos 2000) were quantified in terms of blockiness of the rock mass defined by RQD (Deere, 1963) and Surface discontinuity condition represented by joint condition ( $J_{cond}$  89) defined by Bieniawski (1989). The value of GSI is given by sum of these two scales by a simple expression (Hoek et al., 2013). This modified chart not only have quantitative scales but could also be utilized for the estimation of GSI values from direct visual observations of rock conditions in the field.

Beside intact and jointed rock mass, Berisavljevic et al. (2018) have also measured GSI for weathering induced failures of the heterogeneous fissile rock mass containing sandstone and shale exposed in excavated strata. Similarly, Prihutama and Fahmi (2018) have determined GSI value of 80 with good fracture surface condition and uninterrupted rock mass structure of other rock mass for slope stability analysis of a pillow lava slope. However, there are other views also which considers the algebraic equations linked to GSI as absurd (Barton 2010).

SMR though most widely applied classification system has some limitations in case of closely jointed rock masses and large scale rock slopes (Singh and Goel, 1999). This classification system is not suitable for high slopes with uneven inclination and is basically applicable for structurally controlled slope failures. In order to overcome this limitation another classification system known as slope stability rating (SSR) has been proposed for characterization of slope stability of heavily jointed rock mass (Taheri and Tani, 2007). This system is based on quantitative GSI of Hoek and Brown which has been updated by Sonmez and Ulusay (2002) and non-linear Hoek-Brown failure criterion. It is applicable for non-structurally controlled slope failures. Since some of the major rock slope parameters are not included in GSI, in SSR system, beside the GSI, five additional parameters have been taken into account. These additional parameters included the uniaxial compression strength, rock type, slope excavation method, groundwater and earthquake force. Beside above, in SSR system, a number of design charts are proposed. Each present a set of relationship between the slope height (25 m to 400 m) and SSR values versus the safe slope angle ( $30^\circ$  to  $70^\circ$ ) for a given factor of safety (FoS) 1.0, 1.2, 1.3 and 1.5. Using the above design charts, knowing the SSR value of rock slopes, safe excavation angle versus slope height can be determined for different factor of safety (FoS).

The Q-slope is also an empirical method for rock slope engineering which was developed by supplementing Q-system (Barton et al., 1974). The purpose of this method is to make an assessment of the stability of the excavated rock slope in the field, and make potential adjustment to the slope angles as rock mass condition becomes visible during construction (Barton and Bar, 2015, Bar and Barton, 2017). This method is intended for use in reinforcement free road and railway cuttings or in opencast mines. The Q-slope method utilizes the same six parameters RQD, J<sub>n</sub>, J<sub>r</sub>, J<sub>a</sub>, J<sub>w</sub> and SRF. However, the frictional resistance pair J<sub>r</sub> and J<sub>a</sub> can be applied, if required to the individual potentially unstable wedges. Here, J<sub>w</sub> is termed as J<sub>wice</sub> which takes into account a wider range of environmental conditions. The SRF categories are also slope relevant. In this study, the Q-slope method is applied for all the cut slopes and stable slope angle for each of them is determined.

In the present paper, methodology for simple and rapid assessment of slope stability along road-cut slopes utilizing SMR considering structured slope failure and SSR considering non-structured slope failure, has been verified for its efficacy by applying them to ten road-cut rock slopes faces intercepted along a road section in a reach of 6 km in Kullu area of Himachal Pradesh, India. Design charts proposed under SSR system have been utilized to determine the stability of the cut slopes. The stable slope angles predicted by Q-slope method have been compared with those recommended by SSR system. In the end a comparative analysis of both the

SMR and SSR has also been undertaken to find out the effectiveness of each of the two classification systems.

## Characteristics of the study area

The area selected for study lies in the Kullu district of Himachal Pradesh, India (Fig. 1). It is covered in Survey of India (SOI) toposheet no. 53E/5 between latitude  $31^\circ 51' 00''$  and  $31^\circ 52' 00''$  and longitude  $77^\circ 15' 00''$  and  $77^\circ 20' 00''$  E. The area is accessible from New Delhi via national highway no. NH-44 (New Delhi-Manali highway) up to Bajura hamlet. Further on Bajura-Sheelagarh road via Garsa village along the Hurla nala upstream of Thella village. This is a left bank tributary of river Beas, the main drainage in this region, and joins it near Nagwain.

The study area is located within the Lesser Himalayas of the Kullu region in Himachal Pradesh which is characterized by very rugged topography. The metasedimentary rocks of Manikaran Formation and Banjar Formation belonging to Rampur Group of Proterozoic age with some basic flows falls within a tectonic window with Jutogh and Kullu thrusts as major tectonic features in the area. Bandal granites are the main intrusive within the Rampur Group (Khan, and Prasad, 1996). The main rock types exposed in the area are quartzites, schists, metabasics, granite gneiss, etc. A geological plan of the study area showing major lithounits is given in Fig. 2 (GSI 1999).

## Methodology and technique

The procedure adopted in this study is outline by means of the flowchart given in Fig. 3. As outlined in the flowchart (Fig. 3), step by step procedure adopted to work out stability of the identified cut slopes are discussed in the paragraphs below.

## Field survey and data collection

Field studies were undertaken in the Kullu Himalayas along the Garsa-Sheelagarh road section between Thella and Nijah villages covering a stretch of about 4.5 km. Ten cut slopes have been identified in this stretch, which were excavated during road construction such that major lithounits exposed in the area are covered (Fig. 4). The height of the cut slopes varied from 30 m to 120 m and their lateral extent varied from 40 to 180 m. During the field survey, slope angle and slope directions were also noted.

The rock masses encountered on each slope were fragile having multiple joint sets and rock wedges. The field recording included preparation of data sheets for each cut slope in order to collect input rock mass parameters required for  $RMR_{\text{basic}}$ , SMR, GSI, Q-slope and SSR classification

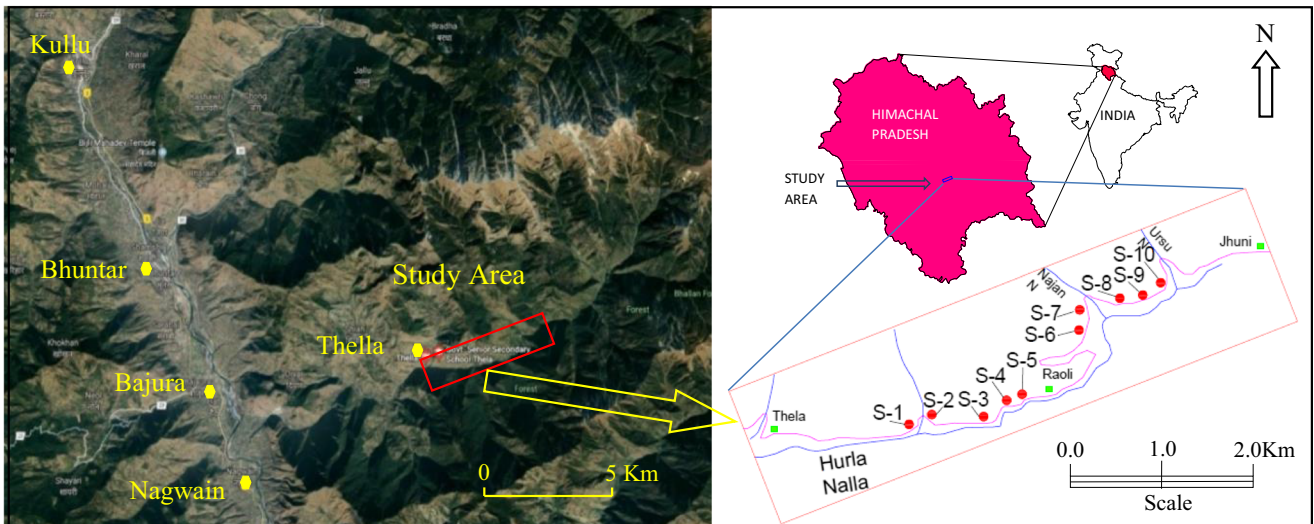


Fig. 1 Location map of study area on Thella-Sheelagarh road section in Kullu area, Himachal Pradesh, India

systems. Joint orientations and important characteristics viz., weathering, persistence, aperture, roughness and infillings were also recorded. Most of the cut slopes evaluated comprises of four major joint sets along with some randomly oriented joints forming polyhedral to rhombohedral blocks of various sizes. The average orientations of major joint sets observed slope wise is given in Table 1. Groundwater conditions associated with each cut slope were also noted during the field survey. Field photographs showing prominent joint sets exposed on the ten cut slopes are shown in Fig. 3.

### Laboratory testing

In order to determine intact rock strength, 5 nos. samples were collected from two to three locations on each of the ten cut slopes. The samples were numbered, trimmed and their dimensions were measured. The point load index tests have been conducted on each sample in dry state as per the procedure outlined in Bureau of Indian Standard IS-8763:1998, ISRM and ASTM standard: D-5731-95 (Fig. 5). Slope wise estimation of uniaxial compressive strength (UCS) is given shown in Table 2.

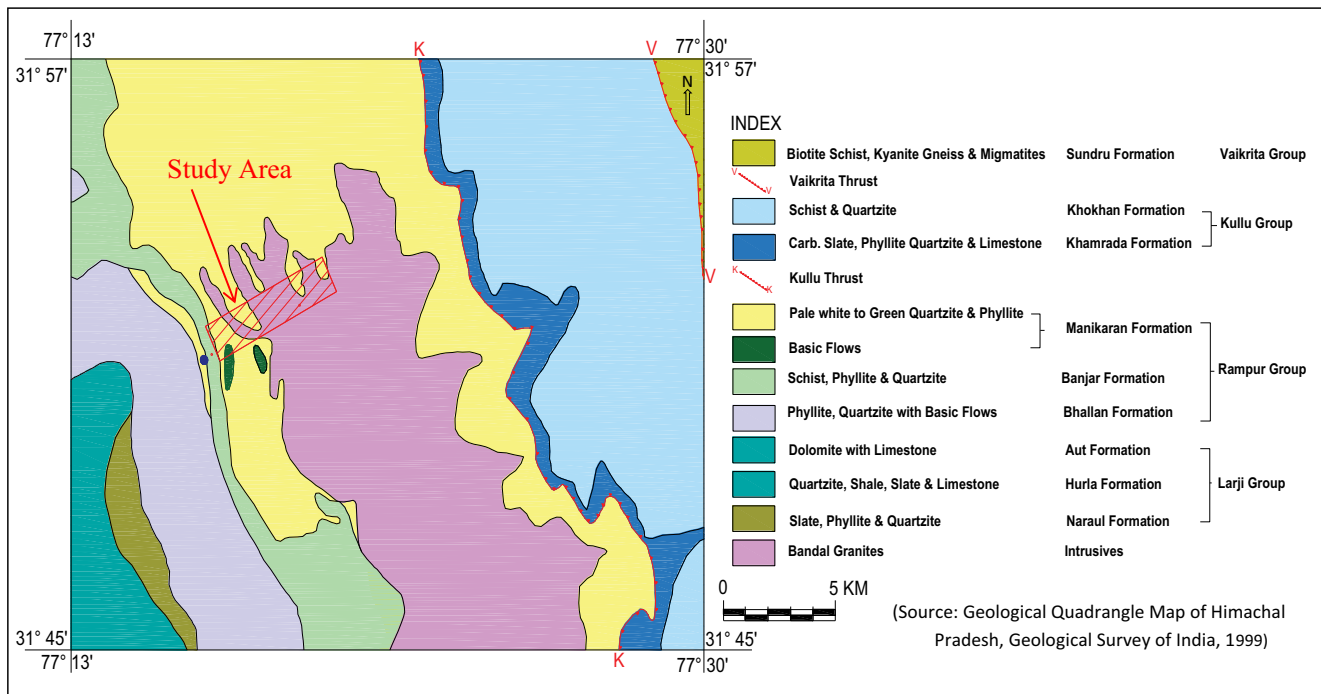
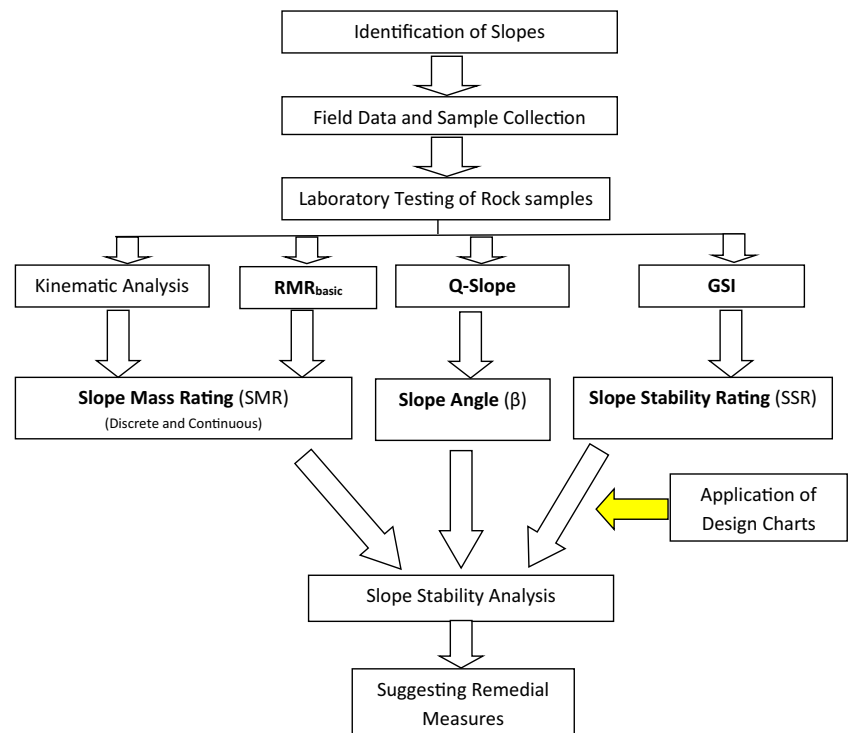


Fig. 2 Geological map of the study area (modified after Geological Survey of India, 1999)

**Fig. 3** Flow diagram showing adopted methodology in the investigation



## Kinematic analysis

In order to determine possible modes of failure, viz., planer, wedge or toppling, stereographic analysis of joints also known as kinematic analysis has been carried out using DIPS software (Rocscience, 2019) (Figs. 6 and 7).

The attitude of various joint sets collected during field survey were plotted on Schmidt stereographic projection on lower hemisphere net and contoured to find out the various pole concentrations. Corresponding to each concentration, representing a major joint set, discontinuity planes were

drawn on the projection net. Plane corresponding to slope face is also plotted on the stereo net along with great circle representing angle of internal friction ( $\phi$ ). Based on the laboratory test results for similar rock types, angle of internal friction ( $\phi$ ) is considered viz.,  $30^\circ$  for metabasics and quartzite,  $25^\circ$  for chlorite schist and  $30^\circ$ – $35^\circ$  for granite gneiss. The relationship between the joint planes and plane representing slope face along with friction cone has been utilized to determine the mode of failure. Figures 8 and 9 represent the various possible wedges and planes vulnerable to failure for each of the ten slopes. Based on the above analysis about 16 joints

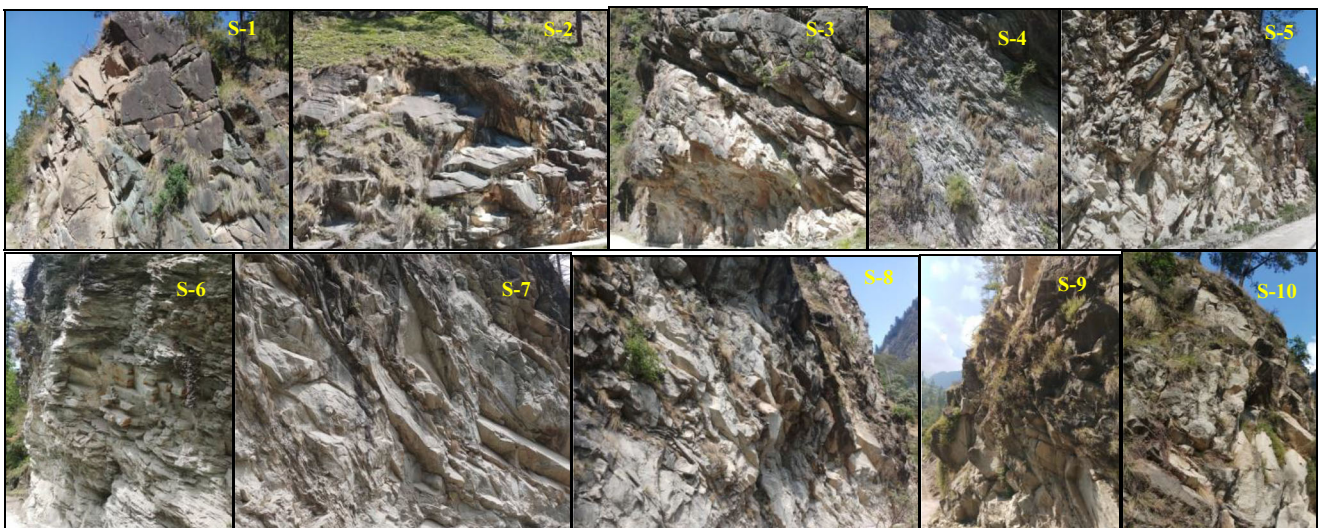


**Fig. 4** Photographs showing ten numbers of selected road-cut slopes (S-1 to S-10) for the study and prominent joint sets exposed on the cut slopes

**Table 1** Joint set data (average orientations) various road-cut rock slopes (Road RD’s start from Thella village)

Slope no.	Location RD* (m)	Foliation joint J-1	Other joint sets				
			J-2	J-3	J-4	J-5	J-6
S-1	5450	050°/70°	140°/70°	320°/60°	200°/50°	350°/65°	150°/30°
S-2	5550	050°/70°	200°/40°	130°/25°	160°/60°	120°/70°	350°/55°
S-3	6850	060°/50°	210°/70°	310°/60°	210°/45°	200°/70°	020°/30°
S-4	7150	040°/60°	200°/70°	310°/60°	170°/60°	110°/45°	
S-5	7300	070°/60°	210°/50°	270°/65°	180°/60°		
S-6	8300	030°/35°	210°/55°	270°/60°	160°/70°		
S-7	9150	030°/45°	200°/30°	310°/65°	160°/45°	270°/60°	
S-8	9400	060°/70°	200°/45°	310°/60°	200°/45°	210°/70°	
S-9	9500	070°/55°	220°/50°	310°/70°	270°/75°	110°/30°	200°/30°
S-10	9660	060°/50°	190°/45°	310°/70°	220°/60°		

(plane failure) and 22 planes (wedge failure) were found to be unstable and prone to sliding. These joints/planes are enumerated in detail while estimating SMR.

**Estimation of RMR<sub>basic</sub> value**

Geotechnical details for each rock slope facet were collected during field survey in form of slope details, joint orientation and characteristics data and rock mass parameters. RMR<sub>basic</sub>

(Bieniawski, 1974) has been estimated by adding five parameters: (i) strength of intact rock; (ii) RQD calculated from volumetric joint count (J<sub>v</sub>) or total number of joints per cubic meter (Palmstrom 2005) using expression RQD = 110 – 2.5 (J<sub>v</sub>); (iii) joint spacing; (iv) joint condition measured in terms of persistence, aperture, roughness, infilling and weathering and lastly (v) water inflow through joints. Water seepage plays a pivotal role in slope stability as it creates pore-pressure and act as lubricant in case of clay filled joints thus facilitating structurally controlled failures. In the present study, during

**Table 2** Estimation of point load index (PLI) and uniaxial compressive strength (UCS) based on laboratory testing

Sample no.	Rock type	De	Failure load in Newton	Un-corrected point load index (MPa)	Size correction factor (F)		Corrected point load index (I <sub>50</sub> ) in MPa	Uniaxial compressive strength (MPa)	Avg. UCS (MPa)
		$\sqrt{De^2}$	P	I <sub>s</sub>	De/50	(De/50) 0.45	F*I <sub>s</sub>	Q <sub>c</sub>	Q <sub>cf</sub>
Site-1A	Metabasics	76.02	19,500	3.37	1.52	1.21	4.07	89.64	89.64
Site-2A	Quartzite	79.41	28,500	4.52	1.59	1.23	5.57	122.44	151.55
Site-2B		79.96	42,500	6.65	1.60	1.24	8.21	180.66	
Site-3A	Quartzite	64.88	18,000	4.28	1.30	1.12	4.81	105.79	107.38
Site-3B		55.36	14,500	4.73	1.11	1.05	4.95	108.98	
Site-4A	Chlorite schist	71.28	12,500	2.46	1.43	1.17	2.89	63.49	84.13
Site-4B		66.44	18,500	4.19	1.33	1.14	4.76	104.77	
Site-5A	Quartzite	73.42	23,500	4.36	1.47	1.19	5.18	114.00	117.75
Site-5B		64.52	20,500	4.92	1.29	1.12	5.52	121.51	
Site-6A	Talc chlorite schist	75.81	12,500	2.17	1.52	1.21	2.62	57.70	77.28
Site-6B		50.68	9500	3.70	1.01	1.01	3.72	81.88	
Site-6C		70.86	18,000	3.58	1.42	1.17	4.19	92.26	
Site-7A	Granite gneiss	57.99	16,500	4.91	1.16	1.07	5.24	115.39	110.25
Site-7B		74.15	22,000	4.00	1.48	1.19	4.78	105.11	
Site-8A	Granite gneiss	89.46	20,500	2.56	1.79	1.30	3.33	73.21	82.96
Site-8B		81.58	22,500	3.38	1.63	1.25	4.21	92.70	
Site-9A	Granite gneiss	59.46	24,000	6.79	1.19	1.08	7.34	161.47	128.12
Site-9B		89.39	26,500	3.32	1.79	1.30	4.31	94.77	
Site-10A	Granite gneiss	77.08	21,000	3.53	1.54	1.22	4.29	94.48	96.02
Site-10B		62.07	15,500	4.02	1.24	1.10	4.43	97.56	

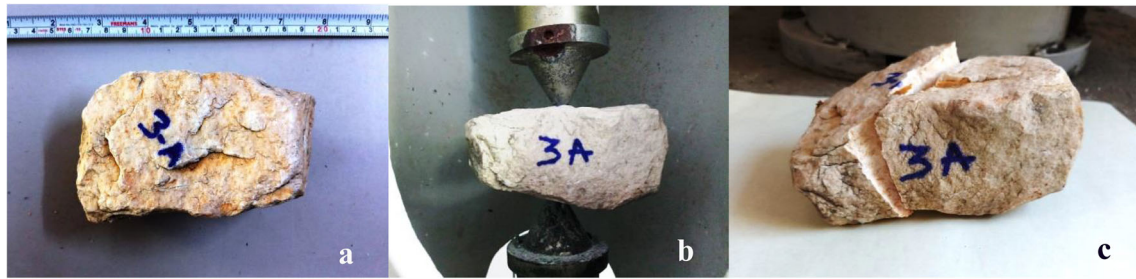


**Fig. 5** (a) Rock sample before testing; (b) testing with rock samples in between platens; (c) post testing failure in rock sample

the time of data collection from site, most of the slope faces have exhibited dry groundwater conditions. Therefore, due consideration shall be required for assessment during rainy season.  $RMR_{basic}$  estimated for each cut slope is shown in Table 3.

In the above estimation, strength of intact rock material is given based on corrected point load index ( $I_{50}$ ) measured in laboratory from the rock samples collected at site (Table 2). All other parameters in this study are based on field estimates.

### Estimation of modified GSI

The GSI is another widely acclaimed rock mass classification system (Hoek and Brown, 1997) that has been applied on slopes using visual interpretation in field. The GSI of the rock mass is determined qualitatively based on the blockiness and the joint surface condition observed in the field. A range of values are assigned based on the chart given by Hoek and Brown (1997). However, since the GSI values are directly used in various failure criteria and other numerical modelling techniques, there is always a requirement of a single value unique for a particular site. In order to achieve this, Sonmez and Ulusay (2002) quantified the GSI chart and proposed two indices: One is Surface Condition Rating (SCR) which is dependent on roughness, weathering and infilling along joints and the other is Structure Rating (SR) which is derived from the volumetric joint count ( $J_v$ ). Thus using the SCR-SR chart (Fig. 8), GSI values can be determined quantitatively for each site.

$$SR = -17.5 \ln(J_v) + 79.8 \quad (1)$$

$$SCR = R_r + R_w + R_f \quad (2)$$

The GSI values thus estimated using the above procedure for ten nos. cut slope is given in Table 4.

A relationship has been worked out between basic RMR values and GSI having correlation coefficient ( $R^2 = 0.84$ ) based on above ten cut slopes (Fig. 9) and which can be expressed as:

$$GSI = 47.3 \ln(RMR) - 112 \quad (3)$$

One of the first approaches to define rock mass condition using GSI was through its application in Hoek-Brown Failure criterion (Hoek et al. 1995) where GSI was derived from RMR (Bieniawski, 1989) using expression:

$$GSI_{1995} = RMR_{89} - 5 \quad (4)$$

Hoek et al. (2013) quantified the original GSI charts (Hoek and Marinos 2000) in terms of the two vertical and horizontal scales representing blockiness of the rock mass defined by RQD (Deere, 1963) and Surface discontinuity condition represented by joint condition ( $J_{cond}$  89) defined by Bieniawski (1989) respectively. The value of GSI is given by sum of these two scales by a simple expression shown below:

$$GSI_{2013} = 1.5 J_{cond89} + RQD/2 \quad (5)$$

A comparative analysis has been done between the GSI values determined for the 10 cut slopes utilizing above three approaches (Fig. 10). The  $GSI_{1995}$  gives the highest values whereas  $GSI_{2013}$  are the lowest for all the slopes.

Basic RMR worked out above shall be utilized for estimation of SMR considering structurally controlled failure while GSI is required for estimation of SSR considering non-structurally controlled slope failure.

### Slope mass rating

SMR is obtained by adding adjustment factors ( $F_1, F_2, F_3$  and  $F_4$ ) to basic RMR proposed by Bieniawski (1989) according to the expression by Romana (1993) as follows:

$$SMR = RMR_{basic} + (F_1 \times F_2 \times F_3) + F_4 \quad (6)$$

$F_1$  reflects parallelism denoted by auxiliary angle 'A' between joint dip direction ( $\alpha_j$ ) and slope direction ( $\alpha_s$ ) in case of plane and toppling failure while line of intersection plunge direction ( $\alpha_i$ ) and slope direction ( $\alpha_s$ ) in case of wedge failure. Its value is 1 which is maximum for  $A < 5^\circ$  (when both are parallel) and 0.15 which is minimum for  $A > 30^\circ$ .  $F_2$  is related to probability of discontinuity shear strength 'B' and depends on dip amount of the joint. The auxiliary angle 'B' is equal to dip of the joint ( $\beta_j$ ) in case of plane failure, plunge of the line of

intersection of two joint forming wedge ( $\beta_i$ ) in case of wedge failure. Its value ranges from 1.0 for 'B' more than  $45^\circ$  to 0.15 for 'B' less than  $20^\circ$ . In case of toppling failure  $F_2$  is 1.0.  $F_3$  depends upon the auxiliary angle 'C' between slope angle ( $\beta_s$ ) and joint dip angle ( $\beta_j$ ) for plane failure and toppling failure and auxiliary angle 'C' between slope angle ( $\beta_s$ ) and plunge

of line of intersection forming the wedge ( $\beta_i$ ) for wedge failure. Its value is 0 (maximum) for  $C > 10^\circ$  to  $-60$  (minimum) for  $C < (-10^\circ)$ .  $F_4$  adjustment factor depends upon method of excavation and its value ranges from +15 for natural slopes to  $-8$  for deficient blasting. The above correction parameters and corresponding ratings are shown in Table 5.

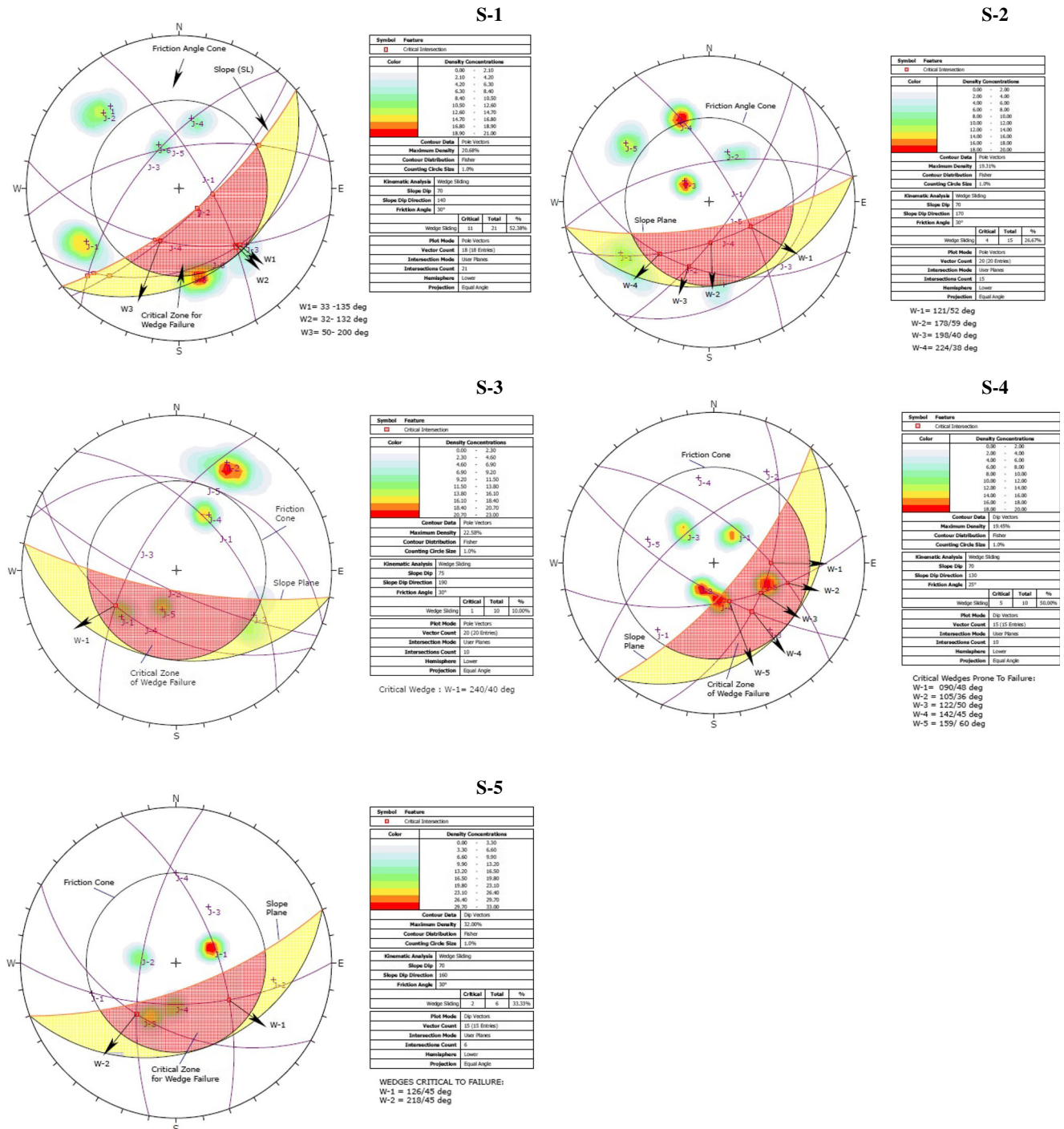
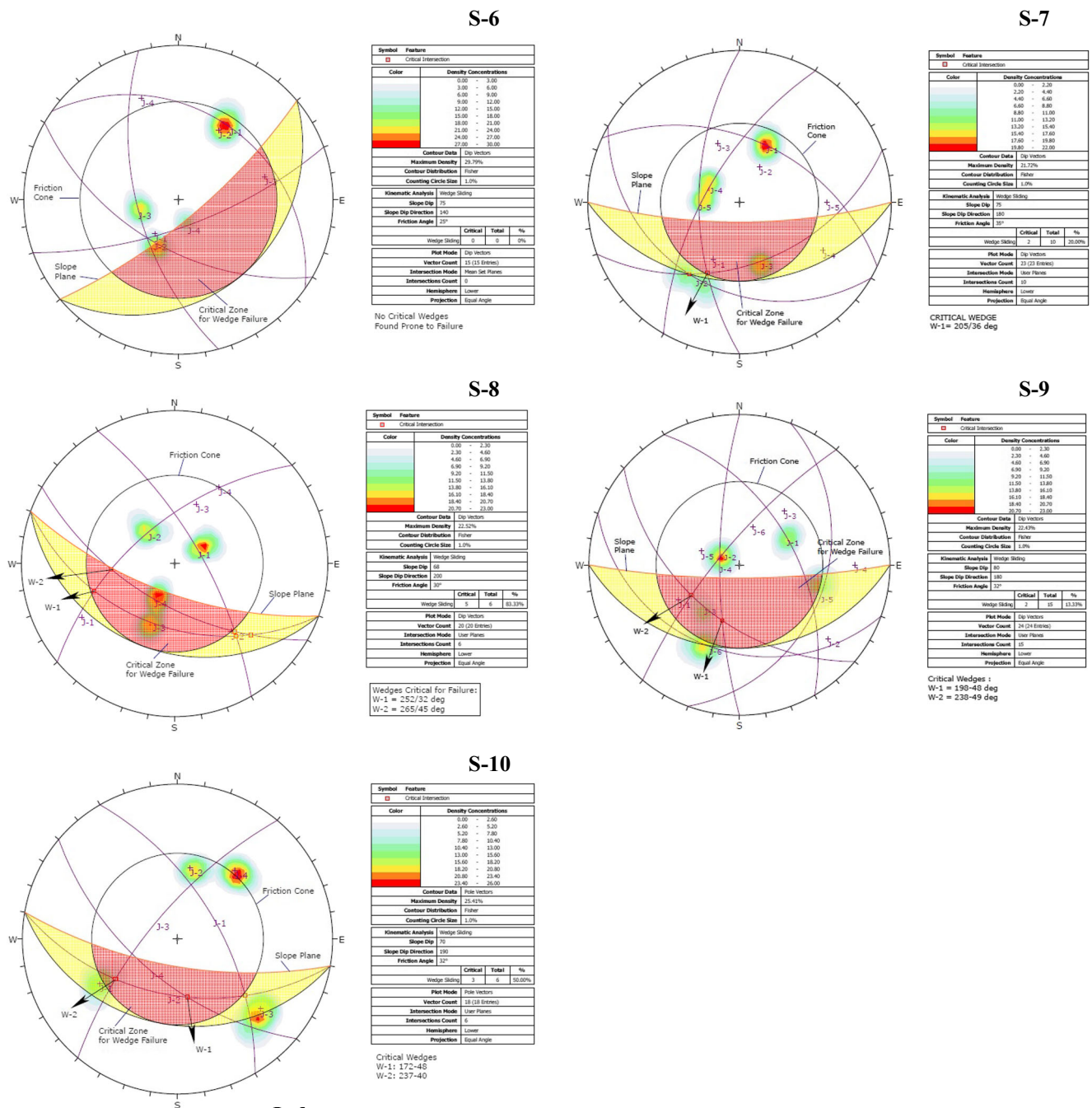


Fig. 6 Kinematic analysis using DIPS software (v7.0, Rocscience Inc.) for determining possible wedges prone to sliding for all the ten slopes evaluated in the study area





**Index**

- S-1 to S-10 :Cut Slopes evaluated using the stereographic projection
- J-1, J-2, J-3..... : Joint sets
- W-1, W-2, W-3 : Possible wedges prone to sliding
- CZ : Critical Zone of Wedge Failure
- SP : Slope Plane
- FC : Friction Cone Circle

Fig. 6 (continued)

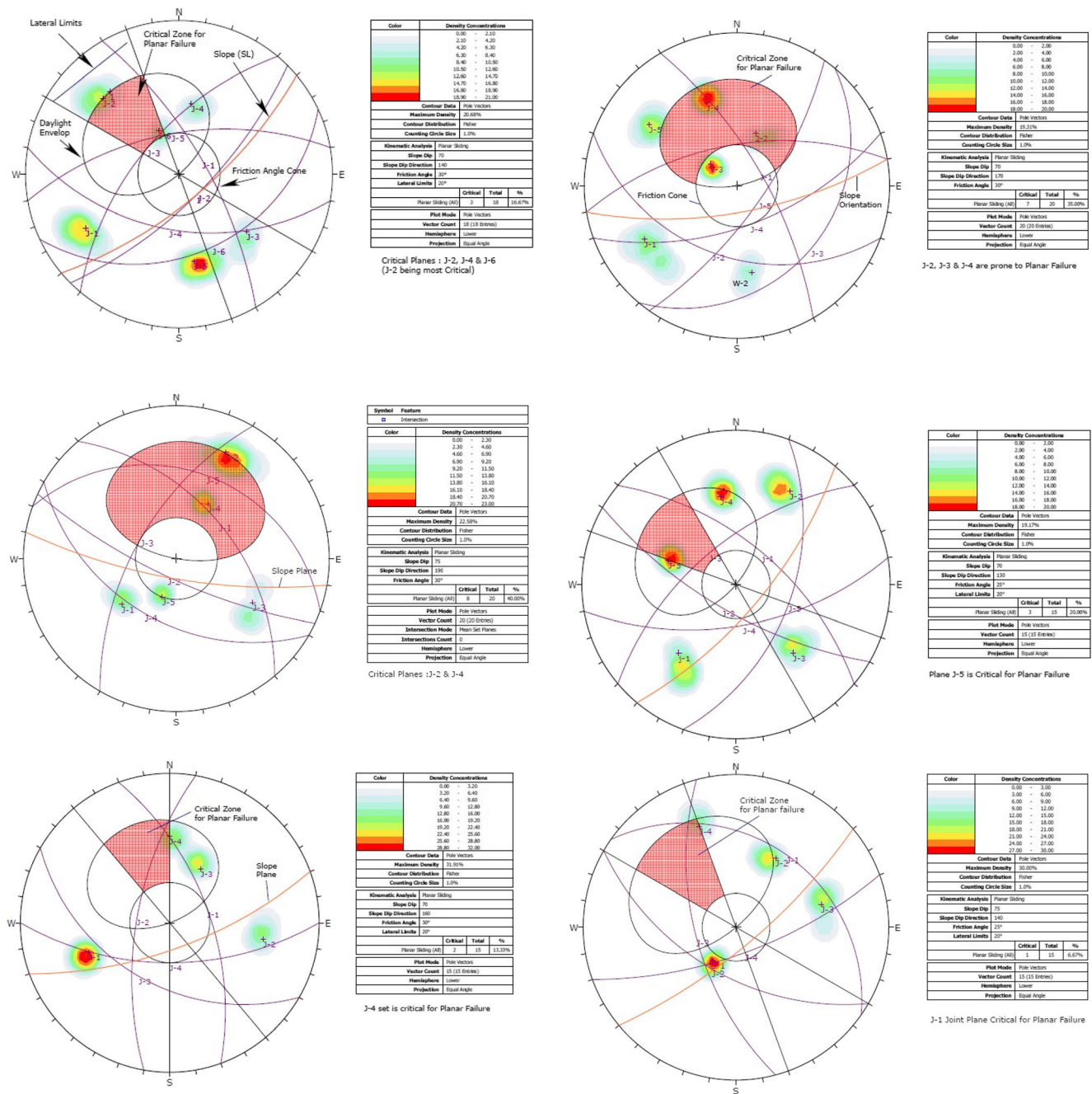
Kinematic analysis has been utilized as discussed in paragraph 5 above to evaluate the failure potential of various

structurally controlled slopes i.e. planer, wedge or toppling failures due to presence of unfavourably oriented joint sets

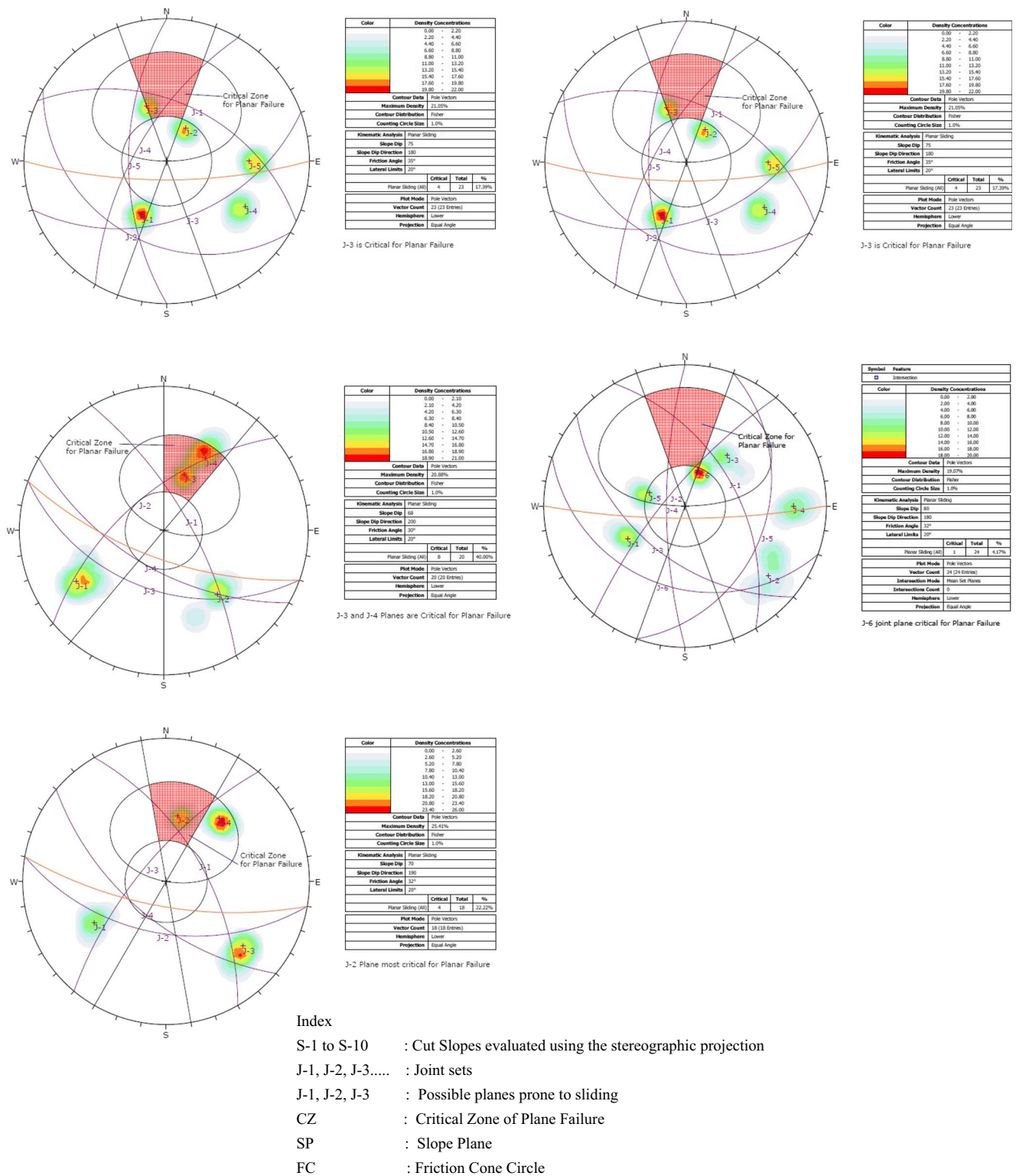
within the rock mass. Planer failure occurs when a joint set dips in the same direction (within  $\pm 20^\circ$ ) as the slope provided the dip amount of joint set is less than the slope inclination angle. Whereas, wedge failure occurs when the line formed by intersection of two joint planes forming wedge shaped rock block, plunges in the direction of slope face. In this case, the plunge amount should be less than the slope angle but greater than friction angle. Toppling failure happen when joint sets dip in the opposite direction of slope by very

steep angle ( $> 75^\circ$ ). Based on kinematic analysis undertaken for all the cut rock slopes as discussed above possible joint planes and wedges prone to sliding were determined for each cut slope. No toppling failure observed on the selected slopes. Considering the type of failure auxiliary angles 'A', 'B' and 'C' were estimated in Table 6 for computing correction factors  $F_1$ ,  $F_2$  and  $F_3$ .

The Correction factors proposed by Romana (1993) for estimation of SMR were discrete in nature. Later on,



**Fig. 7** Kinematic analysis using DIPS software (v7.0, Rocscience Inc.) for determining possible planes prone to sliding for all the ten slopes evaluated in the study area



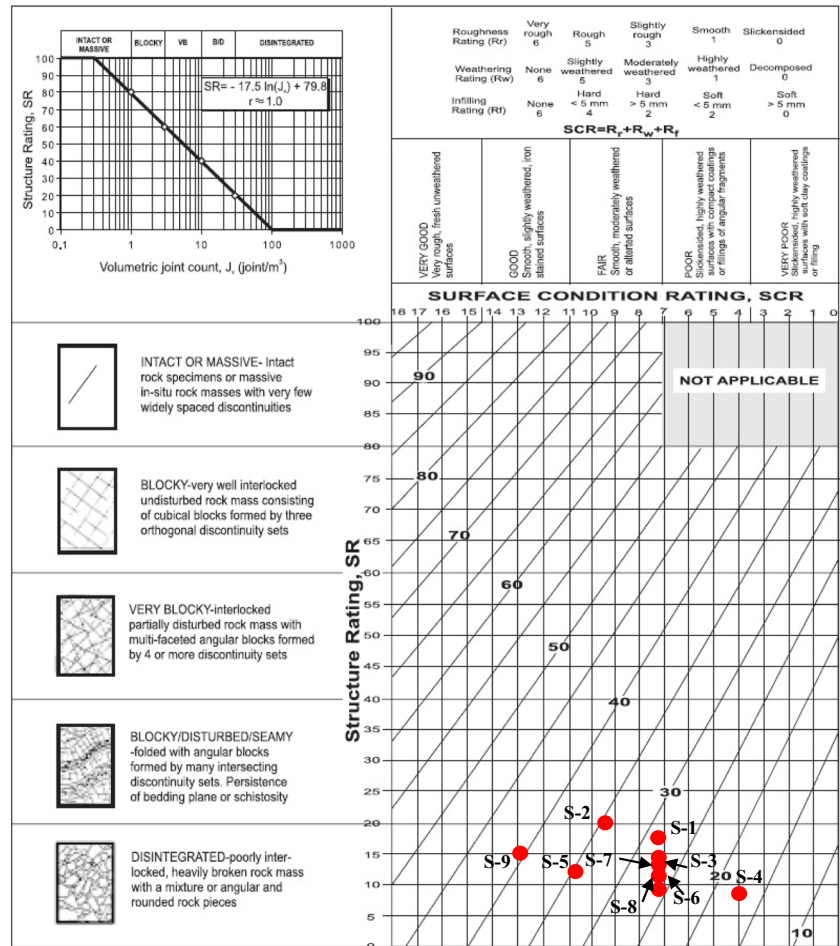
**Index**  
 S-1 to S-10 : Cut Slopes evaluated using the stereographic projection  
 J-1, J-2, J-3..... : Joint sets  
 J-1, J-2, J-3 : Possible planes prone to sliding  
 CZ : Critical Zone of Plane Failure  
 SP : Slope Plane  
 FC : Friction Cone Circle

Fig. 7 (continued)

continuous functions were proposed for calculating adjustment factors (Tomás et al. 2007; Zheng et al., 2016). The continuous slope mass rating (CSMR) reduces the ambiguity

that arises because of the border values and provides better approximation for the stability classes. It is defined by following expressions:

**Fig. 8** Estimation of GSI using quantitative chart (after Sonmez & Ulusay, 2002)



**Fig. 9** Plot showing correlation between  $RMR_{basic}$  and GSI

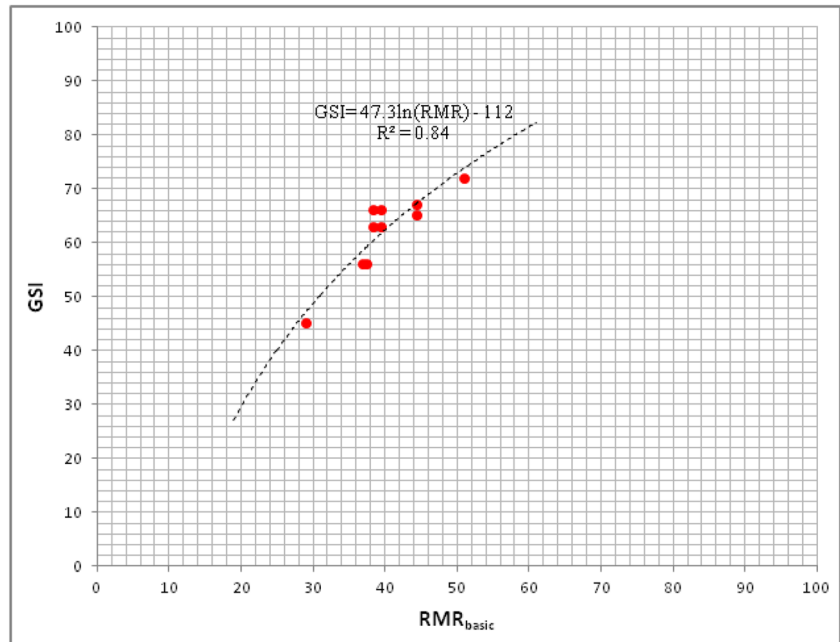


**Table 3** Estimation of  $RMR_{basic}$  based on rating assigned from the rock mass parameters collected at various cut slopes

Slope No.	Rock type	Rock mass description				Joint description					$RMR_{basic}$
		Strength	Water inflow	Joint spacing	RQD	Weathering	Persistence	Aperture	Roughness	Infilling	
S-1	Metabasics	12	15	10	13	5	2	1	3	2	63
S-2	Quartzite	12	15	8	13	5	1	4	3	4	65
S-3	Quartzite	12	15	8	13	5	1	4	3	2	63
S-4	Chlorite schist	7	15	5	8	5	1	1	1	2	45
S-5	Quartzite	12	15	8	13	6	2	4	3	4	67
S-6	Talc chlorite schist	7	15	10	8	5	2	4	3	2	56
S-7	Granite gneiss	12	15	10	13	5	2	4	3	2	66
S-8	Granite gneiss	7	15	10	13	5	1	0	3	2	56
S-9	Granite gneiss	12	15	10	13	6	2	5	5	4	72
S-10	Granite gneiss	12	15	10	13	5	2	4	3	2	66

$$F1 = \frac{16}{25} - \frac{3}{500} \arctan \left( \frac{1}{10} (|A| - 17) \right) \quad (7)$$

$$F2 = \frac{9}{16} + \frac{1}{195} \arctan \left( \frac{17}{100} B - 5 \right) \quad (8)$$

$$F3 = -30 + \frac{1}{3} \arctan C \text{ (Planer and Wedge failure)} \quad (9)$$

$$F3 = -13 - \frac{1}{7} \arctan (C - 120) \text{ (Toppling failure)} \quad (10)$$

A, B and C are auxiliary angles as defined above. Thus, SMR and CSMR are estimated for ten cut slope using both discrete and continuous functions (Table 7). The adjustment factors F1, F2, F3 were determined for both discrete and continuous functions. For the above cut slopes, no toppling failure has been observed therefore estimation has been undertaken for planer and wedge failure only. All the cut slopes selected for this study are located along the road and excavated through mechanical means or by blasting with explosives during the

time of road construction some time back. Therefore, zero value is assigned to F4 for all the cut slopes.

In all the studied ten slopes, 38 potential failure surfaces were determined by kinematic analysis. Out of these 16 are prone to planer and 22 for wedge failures. Similarly, SMR and CSMR values were also worked out for all 38 potential failure surfaces. It is observed that for most of the cut slopes, the SMR values were higher than the CSMR estimated by continuous functions (Fig. 9). The stability classes for all the slopes have been defined and associated failure potential (FI) could be worked out from respective SMR (Table 8).

Based on the stability classes defined in slope mass rating system (Romana, 1985), the SMR classes have been assigned to all the studied cut slopes and stability and potential type of failures has been worked out from the kinematic analysis (Table 9). SMR value of most unfavourable orientation i.e. lowest SMR value observed for each slope is considered to work out the rock mass class and accordingly stability and potential type of failure is determined.

The above analysis has been very effective in evaluating the stability of cut slopes characterized by structurally controlled failures. The kinematic analysis has been significantly useful in indicating the probable plane of failure and type of movement. The potential planes and wedges worked out through above analysis were verified at site also subsequently and found that even though these are not the only failure surfaces but invariably most of the failure has occurred along these potential planes.

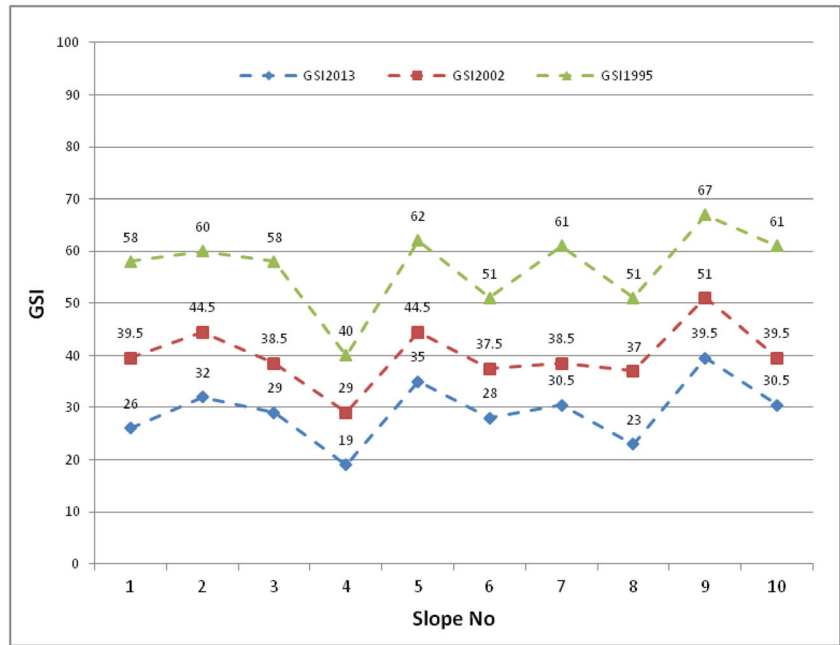
## Slope stability rating

Application of SMR system considers the impact of structurally controlled failures for evaluating slope stability. However, application of this system for closely jointed rock masses and large scale rock slopes has considerable

**Table 4** Estimation of geological strength index (GSI) (Sonmez and Ulusay, 2002)

Slope	$J_v$	$R_r$	$R_w$	$R_f$	SR	SCR	GSI
S-1	16	3	5	2	10	31.28	39.0
S-2	14	3	5	4	12	33.62	37.5
S-3	19	3	5	2	10	28.27	45.0
S-4	25	2	3	2	7	23.47	29.0
S-5	21	3	6	4	13	26.52	44.5
S-6	24	3	5	2	10	24.93	37.5
S-7	20	3	5	2	10	27.37	38.5
S-8	22	3	5	2	10	25.71	38.0
S-9	18	5	6	4	15	29.22	51.0
S-10	17	3	5	2	10	30.22	39.5

**Fig. 10** Comparative plot of GSI1995 (Hoek et al., 1995), GSI2002 (Sonmez & Ulusay, 2002) & GSI2013 (Hoek et al., 2013)



limitations. As the SMR system is inherently dependent upon joint orientation parameters which are difficult to ascertain in very closely jointed or crushed rock masses with several joint sets and also in rock masses with random joints with low persistence and not so clear orientation. Therefore, effectiveness of SMR system is reduced in such type of rock masses.

Another rock mass classification system called SSR has been developed by Taheri et al. (2006) based on some case studies in Iran and further modified by Taheri and Tani (2007) to meet the requirement of closely jointed, large scale and non-structurally controlled slopes. This system is based on modified GSI (Sonmez and Ulusay, 2002) and Hoek-Brown

failure criterion. In GSI system, some of the major slope stability parameters are not included therefore beside GSI, in the SSR system; five additional parameters are considered viz., UCS, rock type, slope excavation method, ground water and earthquake forces. SSR system includes some simple design charts which describe the relationship between the rock slope height and the SSR values versus the stable slope angle, for different factors of safety. These charts can be utilized to design safe slope angle at the same time may also be utilized to validate the stability of existing cut slopes.

The SSR is obtained from modified GSI by adding five additional parameters which affect the stability of fractured rock slopes as follows:

**Table 5** Adjustment factors for SMR proposed by Romana (1985) and modified by Anbalagan et al. (1992)

Type of failure	Relation	Very favourable	Favourable	Fair	Unfavourable	Very unfavourable
Planer Wedge	$A = \alpha i - \alpha s$	$> 30^\circ$	$30^\circ - 20^\circ$	$20^\circ - 10^\circ$	$10^\circ - 5^\circ$	$< 5^\circ$
Toppling	$A = \alpha i - \alpha s 180 - \alpha$					
Adj. factor	F1	0.15	0.40	0.70	0.85	1.00
Planer Wedge	$B = \beta j$ $B = \beta i$	$< 20^\circ$	$20^\circ - 30^\circ$	$30^\circ - 35^\circ$	$35^\circ - 45^\circ$	$> 45^\circ$
Adj. factor	F2	0.15	0.40	0.70	0.85	1.00
Toppling	F2	1.0				
Planer Wedge	$C = \beta j - \beta s$ $C = \beta i - \beta s$	$> 10^\circ$	$10^\circ - 0^\circ$	$0^\circ$	$0^\circ (-10^\circ)$	$< (-10^\circ)$
Toppling	$C = \beta j + \beta s$	$< 110^\circ$	$110^\circ - 120^\circ$	$> 120^\circ$	-	-
Adj. Factor	F3	0	-6	-25	-50	-60
<b>Excavation method</b>		<b>Natural slope</b>	<b>Pre-splitting</b>	<b>Smooth blasting</b>	<b>Blasting or mechanical</b>	<b>Deficient blasting</b>
Adj. factor	F4	+15	+10	+8	0	-8

**Table 6** Input parameters for estimation of slope mass rating (SMR)

Slope no.	RMR <sub>basic</sub>	Failure type	Slope		Discontinuity			Auxiliary angle		
			$\alpha_s$	$\beta_s$	Plane/Line	$\alpha_j/\alpha_i$	$\beta_j/\beta_i$	A	B	C
S-1	63	Planer	140 <sup>0</sup>	70 <sup>0</sup>	J-2	150 <sup>0</sup>	35 <sup>0</sup>	10 <sup>0</sup>	35 <sup>0</sup>	-35 <sup>0</sup>
		Planer	140 <sup>0</sup>	70 <sup>0</sup>	J-4	190 <sup>0</sup>	45 <sup>0</sup>	50 <sup>0</sup>	45 <sup>0</sup>	-25 <sup>0</sup>
		Planer	140 <sup>0</sup>	70 <sup>0</sup>	J-6	130 <sup>0</sup>	35 <sup>0</sup>	10 <sup>0</sup>	35 <sup>0</sup>	-35 <sup>0</sup>
		Wedge	140 <sup>0</sup>	70 <sup>0</sup>	W-1	135 <sup>0</sup>	33 <sup>0</sup>	05 <sup>0</sup>	33 <sup>0</sup>	-37 <sup>0</sup>
		Wedge	140 <sup>0</sup>	70 <sup>0</sup>	W-2	132 <sup>0</sup>	32 <sup>0</sup>	08 <sup>0</sup>	32 <sup>0</sup>	38 <sup>0</sup>
		Wedge	140 <sup>0</sup>	70 <sup>0</sup>	W-3	200 <sup>0</sup>	50 <sup>0</sup>	60 <sup>0</sup>	50	-20 <sup>0</sup>
S-2	65	Planer	170 <sup>0</sup>	70 <sup>0</sup>	J-2	200 <sup>0</sup>	45 <sup>0</sup>	30 <sup>0</sup>	45 <sup>0</sup>	-25 <sup>0</sup>
		Planar	170 <sup>0</sup>	70 <sup>0</sup>	J-3	120 <sup>0</sup>	25 <sup>0</sup>	50 <sup>0</sup>	25 <sup>0</sup>	-45 <sup>0</sup>
		Planar	170 <sup>0</sup>	70 <sup>0</sup>	J-4	160 <sup>0</sup>	65 <sup>0</sup>	10 <sup>0</sup>	65 <sup>0</sup>	-05 <sup>0</sup>
		Wedge	170 <sup>0</sup>	70 <sup>0</sup>	W-1	121 <sup>0</sup>	52 <sup>0</sup>	49 <sup>0</sup>	52 <sup>0</sup>	-18 <sup>0</sup>
		Wedge	170 <sup>0</sup>	70 <sup>0</sup>	W-2	178 <sup>0</sup>	59 <sup>0</sup>	08 <sup>0</sup>	59 <sup>0</sup>	-11 <sup>0</sup>
		Wedge	170 <sup>0</sup>	70 <sup>0</sup>	W-3	198 <sup>0</sup>	40 <sup>0</sup>	28 <sup>0</sup>	40 <sup>0</sup>	-30 <sup>0</sup>
S-3	63	Wedge	170 <sup>0</sup>	70 <sup>0</sup>	W-4	224 <sup>0</sup>	38 <sup>0</sup>	54 <sup>0</sup>	38 <sup>0</sup>	-32 <sup>0</sup>
		Planer	190 <sup>0</sup>	75 <sup>0</sup>	J-2	220 <sup>0</sup>	70 <sup>0</sup>	30 <sup>0</sup>	70 <sup>0</sup>	-05 <sup>0</sup>
		Planar	190 <sup>0</sup>	75 <sup>0</sup>	J-4	210 <sup>0</sup>	45 <sup>0</sup>	20 <sup>0</sup>	45 <sup>0</sup>	30 <sup>0</sup>
		Wedge	190 <sup>0</sup>	75 <sup>0</sup>	W-1	240 <sup>0</sup>	40 <sup>0</sup>	50 <sup>0</sup>	40 <sup>0</sup>	-35 <sup>0</sup>
S-4	45	Planer	130 <sup>0</sup>	70 <sup>0</sup>	J-5	110 <sup>0</sup>	50 <sup>0</sup>	20 <sup>0</sup>	50 <sup>0</sup>	-20 <sup>0</sup>
		Wedge	130 <sup>0</sup>	70 <sup>0</sup>	W-1	090 <sup>0</sup>	48 <sup>0</sup>	40 <sup>0</sup>	48 <sup>0</sup>	-22 <sup>0</sup>
		Wedge	130 <sup>0</sup>	70 <sup>0</sup>	W-2	105 <sup>0</sup>	36 <sup>0</sup>	25 <sup>0</sup>	36 <sup>0</sup>	-34 <sup>0</sup>
		Wedge	130 <sup>0</sup>	70 <sup>0</sup>	W-3	122 <sup>0</sup>	50 <sup>0</sup>	08 <sup>0</sup>	50 <sup>0</sup>	-20 <sup>0</sup>
		Wedge	130 <sup>0</sup>	70 <sup>0</sup>	W-4	142 <sup>0</sup>	45 <sup>0</sup>	12 <sup>0</sup>	45 <sup>0</sup>	-25 <sup>0</sup>
		Wedge	130 <sup>0</sup>	70 <sup>0</sup>	W-5	159 <sup>0</sup>	60 <sup>0</sup>	29 <sup>0</sup>	60 <sup>0</sup>	-10 <sup>0</sup>
S-5	67	Planer	160 <sup>0</sup>	70 <sup>0</sup>	J-4	180 <sup>0</sup>	60 <sup>0</sup>	20 <sup>0</sup>	60 <sup>0</sup>	-10 <sup>0</sup>
		Wedge	160 <sup>0</sup>	70 <sup>0</sup>	W-1	126 <sup>0</sup>	45 <sup>0</sup>	34 <sup>0</sup>	45 <sup>0</sup>	-25 <sup>0</sup>
		Wedge	160 <sup>0</sup>	70 <sup>0</sup>	W-2	218 <sup>0</sup>	45 <sup>0</sup>	58 <sup>0</sup>	45 <sup>0</sup>	-25 <sup>0</sup>
S-6	56	Planer	140 <sup>0</sup>	75 <sup>0</sup>	J-4	160 <sup>0</sup>	70 <sup>0</sup>	20 <sup>0</sup>	70 <sup>0</sup>	-05 <sup>0</sup>
S-7	66	Planer	180 <sup>0</sup>	75 <sup>0</sup>	J-3	160 <sup>0</sup>	45 <sup>0</sup>	20 <sup>0</sup>	45 <sup>0</sup>	-30 <sup>0</sup>
		Wedge	180 <sup>0</sup>	75 <sup>0</sup>	W-1	205 <sup>0</sup>	36 <sup>0</sup>	25 <sup>0</sup>	36 <sup>0</sup>	-39 <sup>0</sup>
S-8	56	Planer	200 <sup>0</sup>	68 <sup>0</sup>	J-3	200 <sup>0</sup>	40 <sup>0</sup>	00 <sup>0</sup>	40 <sup>0</sup>	-28 <sup>0</sup>
		Planar	200 <sup>0</sup>	68 <sup>0</sup>	J-4	210 <sup>0</sup>	70 <sup>0</sup>	10 <sup>0</sup>	70 <sup>0</sup>	02 <sup>0</sup>
		Wedge	200 <sup>0</sup>	68 <sup>0</sup>	W-1	252 <sup>0</sup>	32 <sup>0</sup>	52 <sup>0</sup>	32 <sup>0</sup>	-36 <sup>0</sup>
		Wedge	200 <sup>0</sup>	68 <sup>0</sup>	W-2	265 <sup>0</sup>	45 <sup>0</sup>	65 <sup>0</sup>	45 <sup>0</sup>	-23 <sup>0</sup>
S-9	72	Planer	180 <sup>0</sup>	80 <sup>0</sup>	J-6	200 <sup>0</sup>	30 <sup>0</sup>	20 <sup>0</sup>	30 <sup>0</sup>	-50 <sup>0</sup>
		Wedge	180 <sup>0</sup>	80 <sup>0</sup>	W-1	198 <sup>0</sup>	48 <sup>0</sup>	18 <sup>0</sup>	48 <sup>0</sup>	-32 <sup>0</sup>
		Wedge	180 <sup>0</sup>	80 <sup>0</sup>	W-2	238 <sup>0</sup>	44 <sup>0</sup>	58 <sup>0</sup>	44 <sup>0</sup>	-36 <sup>0</sup>
S-10	66	Planer	190 <sup>0</sup>	65 <sup>0</sup>	J-2	190 <sup>0</sup>	45 <sup>0</sup>	00 <sup>0</sup>	45 <sup>0</sup>	-20 <sup>0</sup>
		Wedge	190 <sup>0</sup>	65 <sup>0</sup>	W-1	172 <sup>0</sup>	48 <sup>0</sup>	18 <sup>0</sup>	48 <sup>0</sup>	-17 <sup>0</sup>
		Wedge	190 <sup>0</sup>	65 <sup>0</sup>	W-2	237 <sup>0</sup>	40 <sup>0</sup>	47 <sup>0</sup>	40 <sup>0</sup>	-25 <sup>0</sup>

$$SSR = GSI + P_1 + P_2 + P_3 + P_4 + P_5 \quad (9)$$

GSI quantitatively estimated in Table 4 above utilizing the modified GSI chart proposed by Sonmez and Ulusay (2002) (Fig. 7) has been considered in estimation of SSR for all the ten rock cut slopes. All the five parameters  $P_1$ ,  $P_2$ ,  $P_3$ ,  $P_4$  and  $P_5$  are evaluated as discussed below. Respective rating values

of all the five parameters are described in Table 10 given by Taheri et al. (2006).

$P_1$  refers to the UCS of the intact rock. It has been determined from point load index (PLI) tests conducted on the rock lump samples in the laboratory, collected from all the slopes under study as outlined in paragraph 4 above. As per Taheri (2012), PLI test is most appropriate method to estimate the compressive

**Table 7** Estimation of slope mass rating (SMR) from input parameters using discrete values (after Romana, 1993) and continuous functions (after Tomas et al., 2007)

Slope no.	Plane/line	Coefficients						Excavation method		SMR	CSMR
		F <sub>1</sub>		F <sub>2</sub>		F <sub>3</sub>		F <sub>4</sub>			
		Disct	Cont.	Disct.	Cont.	Disct.	Cont.	Disct	Cont.		
S-1	J-2	0.70	0.85	0.70	0.79	-60.00	-59.45	0	0	34	23
	J-4	0.15	0.20	0.85	0.92	-60.00	-59.24	0	0	55	52
	J-6	0.70	0.85	0.70	0.79	-60.00	-59.45	0	0	34	23
	W-1	0.85	0.94	0.70	0.72	-60.00	-59.48	0	0	27	22
	W-2	0.85	0.89	0.70	0.68	-60.00	-59.50	0	0	27	27
	W-3	0.15	0.18	1.00	0.94	-60.00	-59.05	0	0	54	53
S-2	J-2	0.15	0.33	0.85	0.92	-60.00	-59.24	0	0	57	47
	J-3	0.15	0.20	0.40	0.37	-60.00	-59.58	0	0	61	61
	J-4	0.70	0.85	1.00	0.98	-60.00	-59.23	0	0	30	18
	W-1	0.15	0.20	1.00	0.95	-60.00	-59.94	0	0	56	54
	W-2	0.85	0.89	1.00	0.97	-60.00	-59.27	0	0	14	15
	W-3	0.40	0.35	0.85	0.88	-60.00	-59.36	0	0	45	47
S-3	W-4	0.15	0.19	0.85	0.85	-60.00	-59.40	0	0	57	55
	J-2	0.15	0.33	1.00	0.98	-50.00	-56.23	0	0	55	45
	J-4	0.40	0.54	0.85	0.92	-20.00	-29.35	0	0	43	34
	W-1	0.15	0.20	0.85	0.88	-60.00	-59.45	0	0	55	53
S-4	J-5	0.40	0.54	1.00	0.94	-60.00	-59.05	0	0	21	15
	W-1	0.15	0.24	1.00	0.93	-60.00	-59.13	0	0	36	32
	W-2	0.40	0.41	0.85	0.81	-60.00	-59.44	0	0	25	25
	W-3	0.85	0.89	1.00	0.94	-60.00	-59.05	0	0	00	00
	W-4	0.70	0.80	0.85	0.92	-60.00	-59.24	0	0	09	02
S-5	W-5	0.40	0.34	1.00	0.97	-60.00	-58.10	0	0	21	26
	J-4	0.40	0.54	1.00	0.97	-60.00	-58.10	0	0	43	37
	W-1	0.15	0.28	0.85	0.92	-60.00	-59.24	0	0	59	52
S-6	W-2	0.15	0.18	0.85	0.92	-60.00	-59.24	0	0	59	57
	J-6	0.40	0.54	1.00	0.98	-60.00	-59.23	0	0	36	26
S-7	J-3	0.40	0.54	0.85	0.92	-60.00	-59.36	0	0	46	37
	W-1	0.40	0.41	0.85	0.81	-60.00	-59.51	0	0	46	46
S-8	J-3	1.00	1.00	0.85	0.88	-60.00	-59.32	0	0	05	04
	J-4	0.70	0.85	1.00	0.98	-06.00	-08.86	0	0	52	49
	W-1	0.15	0.20	0.70	0.68	-60.00	-59.47	0	0	50	48
	W-2	0.15	0.17	0.85	0.92	-60.00	-59.17	0	0	48	47
S-9	J-6	0.40	0.54	0.40	0.59	-60.00	-59.62	0	0	56	47
	W-1	0.70	0.61	1.00	0.93	-60.00	-59.40	0	0	24	32
	W-2	0.15	0.18	0.85	0.91	-60.00	-59.47	0	0	58	56
S-10	J-2	1.00	1.00	0.85	0.92	-60.00	-59.05	0	0	05	02
	W-1	0.70	0.61	1.00	0.93	-60.00	-59.88	0	0	14	23
	W-2	0.15	0.21	0.85	0.88	-60.00	-59.24	0	0	48	45

strength of intact rock for assessment of slope stability. The UCS values tabulated in Table 2 have been utilized for defining  $P_1$  for all the ten slopes considered in this study.

$P_2$  refers to rock type occurring on the slope under consideration. Stability analysis results has shown that variation of

the material constant  $m_i$  in Hoek-Brown failure criteria (Hoek and Brown, 2019) which is approximately equal to friction angle of the intact rock, has significant effect on rock slope stability. Dry unit weight of intact rock is the other parameter. These two parameters are considered to classify rock types



**Table 8** Stability classes as per SMR rating (as per Romana, 1985)

SMR	Class	Rock mass description	Stability	Failures	Probability of failure	Support
81–100	I	Very good	Completely stable	None	0.9	None
61–80	II	Good	Stable	Some blocks	0.6	Occasional
41–60	III	Normal	Partially stable	Some joints or many wedges	0.4	Systematic
21–40	IV	Bad	Unstable	Planer or big wedges	0.2	Important corrective
0–20	V	very bad	Completely unstable	Big planer or soil like	0.0	Re-excavation

into six groups (Taheri et al., 2006). Each rock group has associated rating (Table 10) whose value is assigned to  $P_2$ . The rocks encountered in ten rock cut slopes under study are quartzite, chlorite schist, metabasics and granite gneiss. The above rock types are not mentioned in table of rock groups proposed by Taheri (2012). Therefore, based on their  $m_i$  and dry unit weights, the rock encountered in this study viz., quartzite ( $m_i: 20 \pm 3$ ), chlorite schist ( $m_i: 6 \pm 3$ ), metabasics ( $m_i: 25 \pm 3$ ) and granite gneiss ( $m_i: 28 \pm 3$ ) (Hoek et al., 1998) are placed in the appropriate rock groups (Table 11).

$P_3$  refers to slope excavation method which has considerable effect on the stability of rock slopes (Table 10). As all the slopes under consideration in study are located along the road section and ever excavated by manual excavation and blasting through explosives therefore, normal blasting is considered and accordingly zero value is assigned to  $P_3$  for all the cut slopes under consideration (Fig. 11).

$P_4$  refers to the phreatic level of ground water which is the measure of degree of saturation for the rock slope. The saturation is measured as percentage of the ground water level from the bottom of slope with respect to total slope height (Table 10). For all the slopes under consideration, since phreatic ground water level does not intercepts the slope, ground water is considered dry and accordingly zero value is assigned to  $P_4$ .

$P_5$  considers the effect of earthquakes force on the stability of slope. As per the procedure outlined by Taheri (2012), BIS Code (IS 1893-Part 1, 2002) has been referred to determine the horizontal earthquake acceleration at the location of slopes under study. As per the Seismic Zonation map of India given in the BIS code, the area falls under Zone V. The horizontal acceleration ( $\alpha_h$ ) proposed for designing of large civil structures is 0.36 g. For natural slopes 2/3 value of  $\alpha_H$  is required to be considered. Accordingly, a value of 0.24 g has been considered for all the slopes and thus a rating of – 19 is assigned to  $P_5$ .

As per the procedure, by adding GSI with all the parameters  $P_1$  to  $P_5$ , SSR has been estimated for all the ten slopes (Table 12).

### Evaluation of slope stability using design charts proposed in SSR system

In the SSR system, in order to provide useful tool for preliminary design of rock slopes, based on the studied slopes several stability analysis were performed using limit equilibrium code. Several rock slopes were assumed with height ranging from 25 to 400 m and slope angle from 30 to 70 degrees. Different discontinuity and intact rock properties, slope

**Table 9** SMR classification of ten cut slopes according to their stability and potential type of failures

Slope no.	SMR range	Class	Rock mass description	Stability	Failure type	Potential failure planes
S-1	27–55	IV	Bad	Unstable	Planar or big wedges	Wedge failure along N132°/32°
S-2	14–61	V	Very bad	Completely unstable	Big planar or soil like	Planar failure along N160°/65° Wedge failure along N 178°/59°
S-3	34–55	III	Normal	Partially stable	Some joints or many wedges	Planar failure along N 210°/45°
S-4	0–36	V	Very bad	Completely unstable	Big planar or soil like	Wedge failure along N 122°/50° Wedge failure along N142°/45°
S-5	37–59	III	Normal	Partially stable	Some joints or many wedges	Planar failure along 180°/60°
S-6	36	IV	Bad	Unstable	Planar or big wedges	No failures
S-7	46	III	Normal	Partially stable	Some joints or many wedges	Planar failure along N 160°/45°
S-8	4–47	III	Normal	Partially stable	Some joints or many wedges	Planar failure along 200°/40°
S-9	24–58	IV	Bad	Unstable	Planar or big wedges	Wedge failure along 198°/48°
S-10	5–48	V	Very bad	Completely unstable	Big planar or soil like	Planar failure along 190°/45°

**Table 10** Parameters and ratings of slope stability rating (SSR) rock mass classification system (Taheri et al., 2006)

Parameters		Range of values					
<b>P<sub>1</sub></b>	Uniaxial compressive strength (UCS)	0–10	10–25	25–50	50–100	100–150	150–200
	Rating	0	7	18	28	37	43
<b>P<sub>2</sub></b>	Rock type (Table 11)	Group 1	Group 2	Group 3	Group 4	Group 5	Group 6
	Rating	0	4	9	17	20	25
<b>P<sub>3</sub></b>	Slope excavation method	Waste dump	Poor blasting	Normal blasting	Smooth blasting	Pre-splitting	Natural slope
	Rating	– 11	– 4	0	6	10	24
<b>P<sub>4</sub></b>	Groundwater (Groundwater level from bottom of the slope/slope height) * 100	Dry	0–20%	20–40%	40–60%	60–80%	80–100%
	Rating	0	– 1	– 3	– 6	– 14	– 18
<b>P<sub>5</sub></b>	Earthquake force Horizontal acceleration	0	0.15 g	0.20 g	0.25 g	0.30 g	0.35 g
	Rating	0	– 11	– 15	– 19	– 22	– 26

excavation method, ground water condition and earthquake force were considered. The safety factors of slopes with different SSR values were calculated. In this manner, a set of design charts were prepared each present relationship between the slope height and the SSR value versus safe slope angle (between 30° and 70°) and for factor of safety 1.0, 1.2, 1.3 and 1.5 (Taheri et al., 2006) (Fig. 12). From these charts, knowing the SSR value of the rock slope, the safe slope excavation angle for a given slope height can be determined at different factor of safety (Fig. 10).

In study, as the slopes were already excavated cut slopes along the road section about a decade back from the period when this study has been carried out. However, no slaking process had advanced along the slope and these rock cut slopes are not prone to slaking. Therefore, the above design charts have been utilized to perform slope stability analysis by comparing the estimated slope angle with the actual slope angles for different factor of safety (FoS = 1.0, 1.2 and 1.5) as shown in Fig. 10 A, B and C respectively. The SSR values determined for each of the 10 cut slope were plotted w.r.t.

slope height and superimposed on the design charts to evaluate the safe slope angle (Table 13).

Based on the above analysis, it is seen that out of the 10 cut slopes, 6 are stable, 2 are partially stable and 2 are unstable. The slope angles of two unstable cut slopes viz., S-4 and S-6 which are excavated in chlorite schist rock mass are higher than the safe slope angle worked out from the design chart. For the minimum factor of safety of 1.0, the slope angle of these two slopes should be less than 45° and 55° respectively. Otherwise, danger of rock fall and sliding shall always be there.

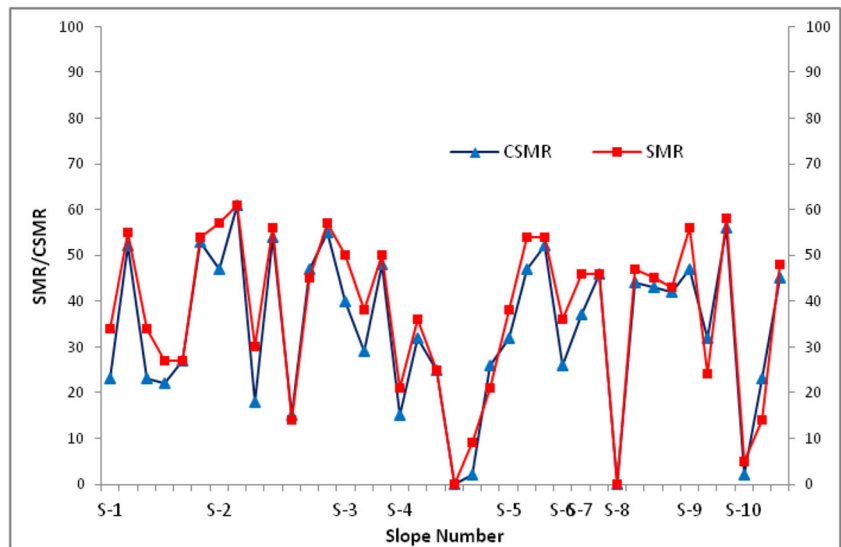
### Q-slope method

Q-slope is an empirical rock slope engineering method for the assessment of the stability of cut slopes excavated in rocks for construction of roads, railways and open cast mining sites (Barton & Bar, 2015). This method is derived from Q-system of rock mass characterization (Barton et al., 1974)

**Table 11** Rock groups defined for SSR classification system (modified after Taheri et al., 2006)

Rock group	Rock type	Name of rocks	m <sub>i</sub> value	Dry unit weight (KN/m <sup>3</sup> )
1	Sedimentary	Clay shale, mudstone, claystone and marl	4	25
2	Metamorphic	Schists and mylonites	6	26.6
3	Sedimentary	Limestone shale, dolomite, limestone, chalk and siltstone	9	27
	Metamorphic	Slate, Phyllite and marble		
4	Sedimentary	Anhydrite and gypsum	16	27.2
	Igneous	Tuff, basalt, breccia, dacite and rhyolite		
5	Sedimentary	Breccia, greywacke, sandstone and conglomerate	20	27.3
	Metamorphic	Hornfels and quartzite		
6	Igneous	Dolerite, obsidian, andesite, norite and agglomerate	28	26.6
	Metamorphic	Granite, granodiorite, diorite, gabbro and metabasics Gneiss		

**Fig. 11** Slope wise plot of SMR versus CSMR for rock cut slope of road section



used for rock exposures, drill cores and tunnels since last four decades. The  $Q'$  parameters (RQD,  $J_n$ ,  $J_a$  and  $J_r$ ) remain unchanged in Q-slope. However, a new method for applying  $J_r/J_a$  ratios to both planes of potential wedges is used with relative orientation weightings for each plane known as orientation factor (O). The term  $J_w$  is represented by  $J_{wice}$  which takes into consideration long term exposure of the rock mass to various climatic and environmental conditions. Here, slope relevant SRF for slope surface conditions, stress-strength ratios and major discontinuities is utilized. Q-slope is developed based on more than 400 case studies of slopes ranging from less than 5 m to more than 250 m in height (Bar & Barton, 2017). It is estimated using the expression:

$$Q\text{-slope} = \frac{RQD}{J_n} \times \left( \frac{J_r}{J_a} \right) O \times \frac{J_{wice}}{SRF_{slope}} \quad (10)$$

### Evaluation of slope stability from Q-slope

In this study, ten road-cut slopes were evaluated w.r.t., each of the above factors defining the Q-slope using respective characterization tables (Barton & Bar, 2015). The joint orientation factor (O-factor) provides orientation adjustment for joints in rock slopes. The set A orientation factor is applied to the most unfavourable joint set. In case of wedges, Set A and set B orientation factor is applied to both sliding planes defining the potentially unstable wedge. The SMR study undertaken above has helped in identifying the most unstable planes and wedges on each rock cut slope. Three cut slopes had wedges while remaining seven had planes as most unstable planes. As the study area is located in lower Himalayas, tropical storms category was selected for estimation of  $J_{wice}$ . The strength reduction factor  $SRF_{slope}$  is obtained by using the most adverse, i.e. maximum of  $SRF_a$  (physical condition),  $SRF_b$

**Table 12** Estimation of slope stability rating (SSR) for ten cut slopes

Slope no.	GSI		Rock type			Slope excavation method			Groundwater		Earthquake force		SSR rating
	Value	P <sub>1</sub>	Value	P <sub>2</sub>	Value	P <sub>3</sub>	Value	P <sub>4</sub>	Value	P <sub>5</sub>			
S-1	39.0	89.64	34	Metabasic	Group 6	25	Normal blasting	0	Dry	0	0.24 g	-19	79.0
S-2	37.5	151.55	45	Quartzite	Group 5	20	Normal blasting	0	Dry	0	0.24 g	-19	83.5
S-3	45.0	107.38	40	Quartzite	Group 5	20	Normal blasting	0	Dry	0	0.24 g	-19	86.0
S-4	29.0	84.13	34	Chlorite schist	Group 2	4	Normal blasting	0	Dry	0	0.24 g	-19	48.0
S-5	44.5	117.75	40	Quartzite	Group 5	20	Normal blasting	0	Dry	0	0.24 g	-19	85.5
S-6	37.5	77.28	34	Talc chlorite schist	Group 2	4	Normal blasting	0	Dry	0	0.24 g	-19	56.5
S-7	38.5	110.25	40	Granite gneiss	Group 6	25	Normal blasting	0	Dry	0	0.24 g	-19	84.5
S-8	38.0	82.96	34	Granite gneiss	Group 6	25	Normal blasting	0	Dry	0	0.24 g	-19	78.0
S-9	51.0	128.12	40	Granite gneiss	Group 6	25	Normal blasting	0	Dry	0	0.24 g	-19	97.0
S-10	39.5	96.02	34	Granite gneiss	Group 6	25	Normal blasting	0	Dry	0	0.24 g	-19	79.5

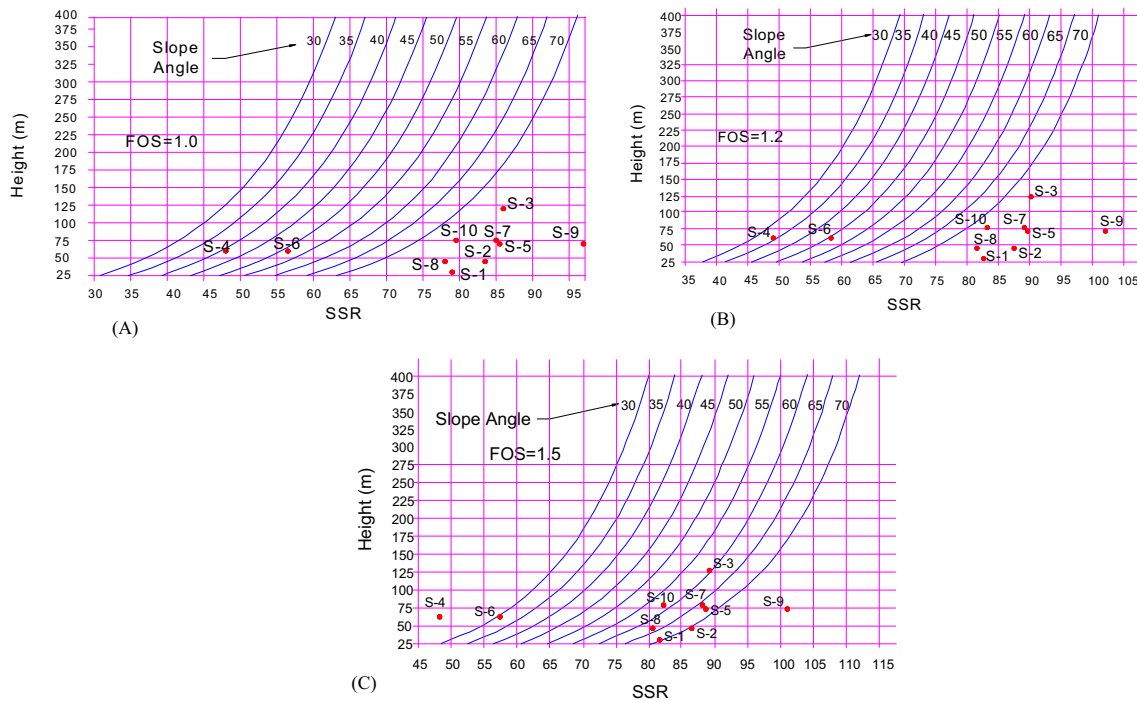


**Fig. 12** SSR versus slope height plot of ten numbers cut slopes superimposed on the SSR design charts for various factor of safety to work out the safe slope angle (a) FoS = 1, (b) FoS = 1.2 and (c) FoS = 1.5

(stress) and  $SRF_c$  (discontinuity orientation). In the above expression, factors, viz.,  $(J_r/J_a)$  and  $SRF_b$ , are affected by slope height. In this study, the slope height varies from 30 to 120 m. The Q-slope estimated utilizing expression 10 for the ten cut slopes is shown in Table 14. The Q-slope values ranges from 0.06 to 4.68. The Q-slope values are plotted against actual excavated slope angle on Q-slope stability chart given by Bar and Barton (2017). It is found that out of the ten slopes, five are stable (S1, S2, S5, S8 and S10), three are quasi-stable (S3, S7 and S9), while two slopes (S4 and S6) were found to be unstable (Fig. 13).

Barton and Bar (2015) derived a simple expression for determining steepest slope angle ( $\beta$ ) not requiring any reinforcement or support applicable for all slope heights. It is given as:

$$\text{Slope angle } (\beta) = 20 \log_{10} Q_{\text{Slope}+} + 65 \tag{11}$$

The above expression has probability of slope failure (PoF) of 1%. Based on Q-slope data from 412 case studies, Bar and Barton (2017) worked out expressions for 15%, 30% and 50% probability of failures. In this study, the same expressions are

**Table 13** Comparison of estimated and actual slope angle to determine the stability of cut slopes

Slope no.	SSR rating	Slope height (m)	Slope angle	Calculated safe slope angle from design charts			Stability condition
				FoS = 1.0	FoS = 1.2	FoS = 1.5	
S-1	79.0	30	70°	> 70°	> 70°	70°	Stable
S-2	83.5	45	70°	> 70°	> 70°	> 70°	Stable
S-3	86.0	120	75°	> 70°	> 70°	60°	Partially stable
S-4	48.0	60	70°	45°	35°	< 30°	Unstable
S-5	85.5	70	70°	> 70°	> 70°	70°	Stable
S-6	56.5	60	72°	55°	50°	35°	Unstable
S-7	84.5	75	70°	> 70°	> 70°	70°	Stable
S-8	78.0	45	65°	> 70°	> 70°	65°	Stable
S-9	97.0	70	75°	> 70°	> 70°	> 70°	Partially stable
S-10	79.5	75	65°	> 70°	> 70°	60°	Stable

**Table 14** Estimation of Q-slope for ten cut slopes

Slope	RQD	Jn	Unstable wedge or plane	Set A	Set B	Set A		Set B		Q-factor		Jwice	SRF slope	Q-slope	
						Jr	Ja	Jr	Ja	Set A	Set B				
						S-1	70	15	132°/32°	W	050°/70°				200°/50°
S-2	75	15	160°/65°	P	160°/65°		3	0.75			0.75		0.5	2.5	3.00
S-3	60	15	210/45	P	210°/45°		3	1			0.75		0.5	2.5	1.80
S-4	47.5	15	122/50	W	200°/70°	310°/60°	1	4	2	1	0.75	0.9	0.3	5	0.06
S-5	57.5	12	180/60	P	180°/60°		3	0.75			0.5		0.5	2.5	1.92
S-6	50	12	160/70	P	160°/70°		1.5	4			0.75		0.3	5	0.07
S-7	65	15	160/45	P	160°/45°		3	1			0.75		0.5	2.5	1.95
S-8	55	15	200/40	P	160°/45°		3	0.75			0.75		0.5	2.5	2.20
S-9	65	15	198/48	W	070°/55°	110°/30°	3	1	2	0.75	0.75	0.9	0.5	2.5	4.68
S-10	67.5	12	190/45	P	190°/45°		3	1			0.5		0.5	2.5	1.69

utilized to work out optimal angles ( $\beta$ ) without any requirements of reinforcement measures for ten cut slopes for the PoF as 1%, 15%, 30% and 50% as shown in Table 15.

### Results and discussions

In this study ten rock cut slopes were identified along a road section of about 5 km stretch covering almost all the lithologies present in the area. All these cut slopes were subjected to stability analysis considering both structurally controlled (non-continuum) and non-structurally controlled (continuum) failures. SMR has been estimated after working

out basic RMR and other adjustment factors required for the study of the selected cut slopes. Both discrete and continuous functions have been applied for the estimation of slope mass rating for all the cut slopes. It has been observed that instability of these cut slopes is basically governed by one or two planes or wedges which are most prone to failure. Such failure planes and wedges have been identified for each cut slope. A comparative study of SMR and CSMR from 38 nos. of potential failure planes in all the cut slopes shows that for almost every failure surface, CSMR value is relatively lower than the SMR. Since SMR index only account for the structurally controlled failures and is not valid for closely jointed rock mass therefore to substantiate this limitation

**Fig. 13** Slope stability prediction using Q-slope stability chart (Bar & Barton 2017)

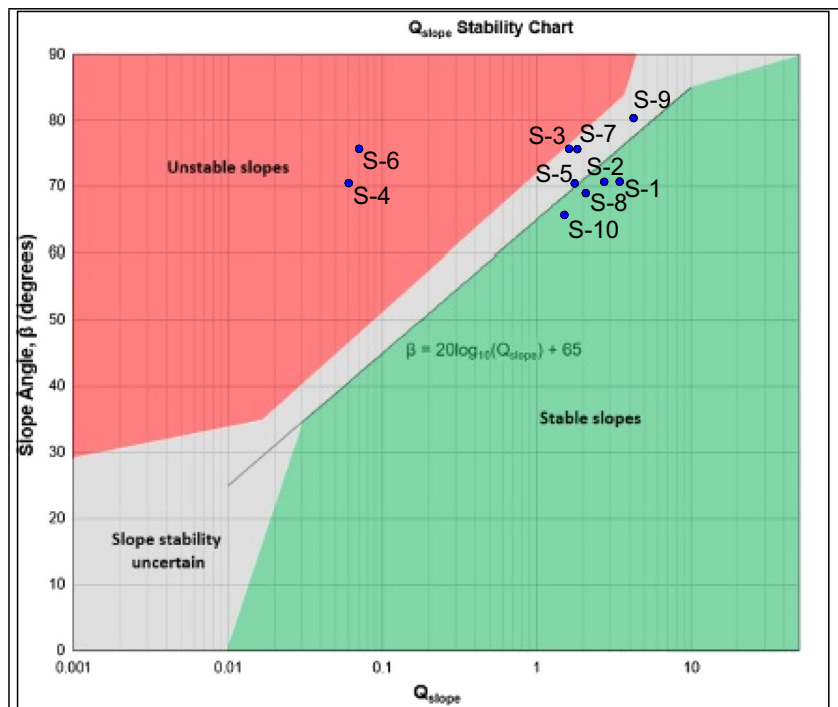


**Table 15** Safe slope angles worked out from Q-slope method for probability of failure (PoF) of 1%, 15%, 30% and 50%

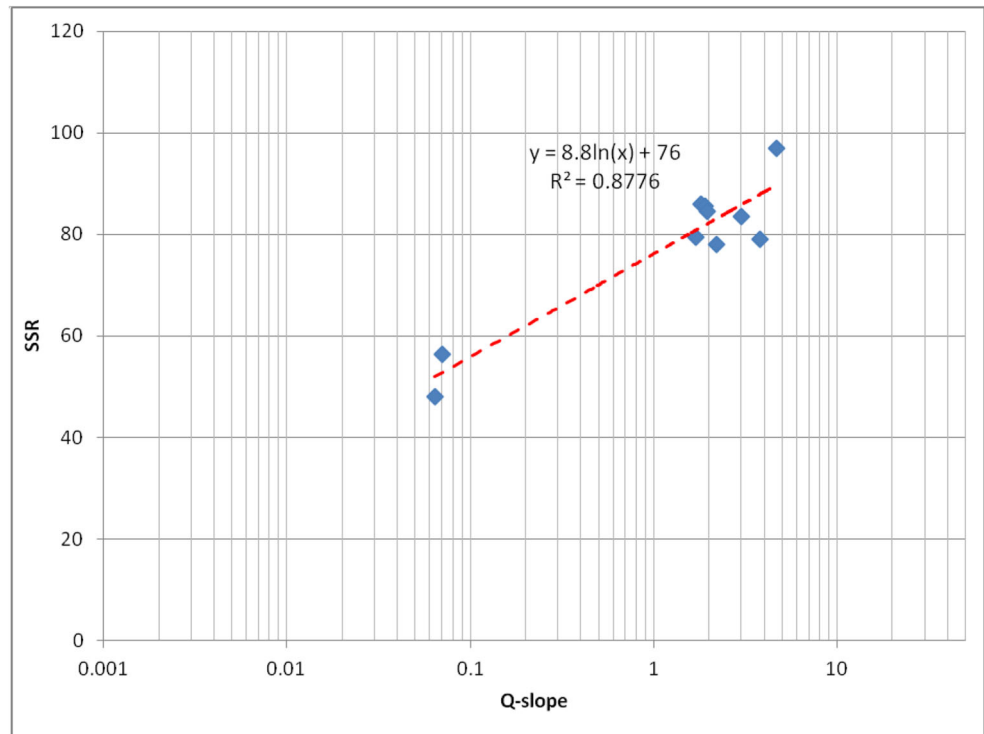
Slope	Actual excavated slope	Q-slope method			
		Safe slope angle (PoF = 1%)	Safe slope angle (PoF = 15%)	Safe slope angle (PoF = 30%)	Safe slope angle (PoF = 50%)
S-1	70	76.55	79.05	82.05	85.05
S-2	70	74.54	77.04	80.04	83.04
S-3	75	70.11	72.61	75.61	78.61
S-4	70	41.14	43.64	46.64	49.64
S-5	70	70.65	73.15	76.15	79.15
S-6	75	41.94	44.44	47.44	50.44
S-7	75	70.80	73.30	76.30	79.30
S-8	68	71.85	74.35	77.35	80.35
S-9	80	78.40	80.90	83.90	86.90
S-10	65	69.54	72.04	75.04	78.04

another classification system known as SSR proposed by Taheri et al. (2006) has also been applied on the selected cut slopes.

SSR rating system incorporates the modified GSI (Sonmez and Ulusay, 2002) along with five other parameters viz., UCS, rock type, excavation method and earthquake force. UCS has been worked out from the point load index test undertaken in laboratory. Rock types encountered in the selected cut slopes were not mentioned in the reference chart provided by Taheri et al., 2006. Therefore, based on the procedure followed by Hoek et al., 1998, considering their  $m_i$  values, the rock types encountered in the slopes were appropriately placed in the

reference table. Earthquake forces in terms of horizontal acceleration for the study area has been worked out from the respective BIS code and seismic zonation map of India. Considering all the parameters, SSR has been estimated for the selected slopes. SSR classification system has proposed several design charts for working out the stability of the cut slopes. The SSR values plotted against slope height has been superimposed on design chart for various factors of safety viz., 1.0, 1.2 and 1.5 respectively. Comparing the observed slope angle and the safe slope angles estimated from the design charts, stability of the respective slopes has been determined.

**Fig. 14** Relationship between Q-slope and SSR for the study area



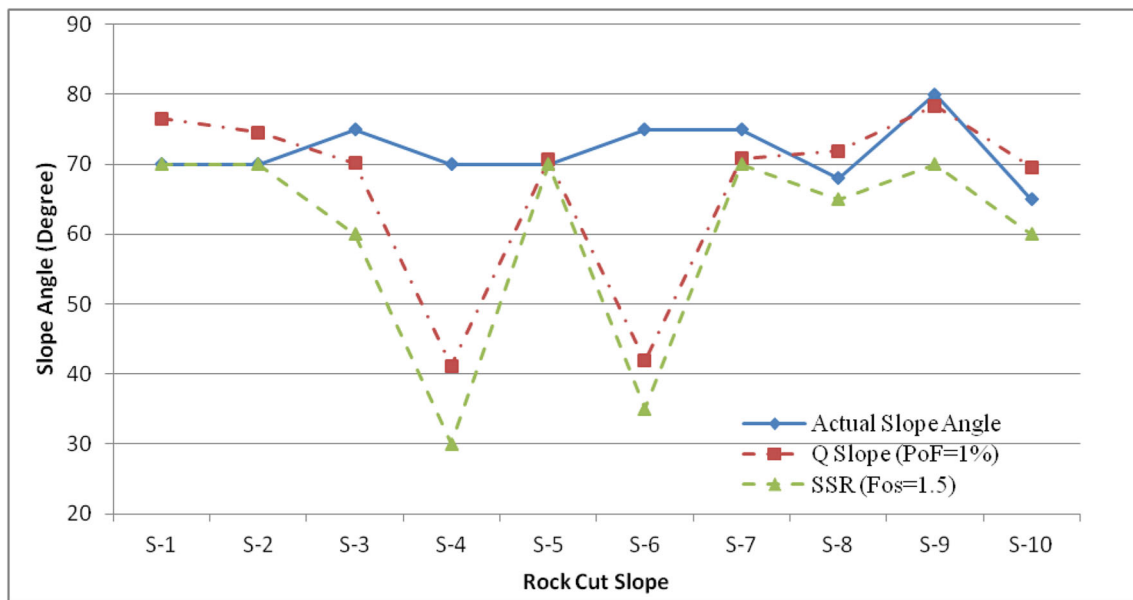


**Fig. 15** Comparison of excavated slope angles with safe slope angles predicted through Q-slope (PoF = 1%) and SSR (FoS = 1.5)

Lastly, Q-slope method is applied on the rock cut slopes to reassess the stability of slopes and work out the steepest safe angle of excavation. The Q-slope values estimated for each cut slopes were plotted on Q-stability plot for respective slope angles of excavated slope to work out their stability. A correlation is established between SSR and Q-slope from the above case study as follows:

$$\text{SSR} = 8.8 \ln Q_{\text{slope}} + 76$$

Even though this expression is based on only limited data set (Fig. 14) but it is giving regression coefficient ( $R^2 = 0.88$ ) which is quite appreciable. However, more data shall be evaluated to firm up this expression in future studies of this area. The safe angle proposed by SSR system for optimum factor of safety (FoE) of 1.5 has been correlated with the safe angle for the above slope cuts for probability of failure (PoE) of 1%. From this comparison, it appears that SSR system proposes much more conservative safe slope angles than Q-slope method (Fig. 15).

## Conclusions

The above case study evaluates the stability of road side cut slopes based on SMR, CSMR, SSR and Q-slope systems of stability analysis methods of rock engineering. The major conclusions of this study are illustrated as follows:

1. Based on analysis, it is observed that out of the 10 selected cut slopes, 2 are completely unstable, 5 are unstable and only 2 are stable.

2. Results suggested that instability of these cut slopes is basically governed by one or two planes or wedges which are most prone to failure.
3. A comparative study of SMR and CSMR from 38 numbers of potential failure planes in all the cut slopes shows that for almost every failure surface, CSMR value is relatively lower than the SMR.
4. The study recommends substantiating limitation of SMR by SSR.
5. As per SSR, the studied rock cut slopes are characterized as out of the 10 selected cut slopes 6 are stable, 2 are partially stable and 2 are unstable.
6. Q-slope method has been applied to work out the stability of slopes. It is found that five slopes are stable, three are quasi-stable while two are unstable.
7. Based on the experience gained through this study, it is worthwhile to mention that while undertaking stability analysis of the cut slopes in mountainous terrain like Himalayas, it shall be prudent to apply both SMR and SSR rating systems simultaneously for comprehensive evaluation of cut slope stability and identification of failure planes.

**Acknowledgements** The first author gratefully acknowledges the financial assistance provided by Department of Atomic Energy – Board of Research in Nuclear Sciences (DAE-BRNS), Mumbai, India (File No. 2013/36/56-BRNS/2447) and Ministry of Earth Sciences (MoES), New Delhi, India (No. 115/IFD/15), in the form of research projects for landslide study in Himalayan region and strength of rocks. The authors are thankful to Director, Indian Institute of Technology (ISM), Dhanbad, India, for his administrative supports.

**Author contributions** The field work and some analysis were carried out by the first author and rest of diagrams and interpretation was made by second author. The 50% parts of paper are contributed by each author.

**Funding** The study was supported by the Ministry of Earth Science under the Project (MoES No. 115/IFD/15) and DAE-BRNS, Mumbai, India (File No. 2013/36/56-BRNS/2447), for landslide study in Himalayan region and strength of rocks.

**Data availability** Availability of data and material (data transparency) and code availability (software application or custom code) are on request basis.

## Compliance with ethical standards

The paper follows the scientific ethics. The authors are happy to provide consent for publication.

**Conflict of interest** The authors declare that they have no conflict of interest.

## References

- Anbalagan R, Sharma S, Raghuvanshi TK (1992) Rock mass stability evaluation using modified SMR approach. In: Proceedings of 6th Nat Symp Rock Mech, Bangalore, India: 258–268
- Barton N (2010) TBM prognoses through hard rock, high stress, or weakness zones, using QTBMs methods with open-gripper or double-shield TBM. Keynote lecture, VII th South American Congress of Rock Mechanics, Lima Peru, pp 5–9
- Barton N, Lien R, Lunde J (1974) Engineering classification of rock masses for design of tunnel support. *Rock Mech* 6:189–236
- Barton N, Bar N (2015) Introducing the Q-slope method and its intended use within civil and mining engineering projects. EUROCK 2015 & 64th Geomechanics Colloquium. Schubert & Kluckner (ed.) ISRM Regional Symposium EUROCK 2015 - Future Development of Rock Mechanics, pp 157–162
- Bar N, Barton N (2017) The Q-slope method for rock slope engineering. *Rock Mech Rock Eng* 50(12):3307–3322
- Basahel H, Mitri H (2017) Application of rock mass classification systems to rock slope stability assessment: a case study. *J Rock Mech Geotech Eng* 9(6):993–1009
- Berisavljevic Z, Berisavljevic D, Rakic D, Zoran Radić Z (2018) Application of geological strength index for characterization of weathering-induced failures. *Gradevinar* 70(10):891–903
- Bieniawski ZT (1974) Geomechanics classification of rock masses and its application in tunnelling. In: Proceedings of 3rd International Congress of Rock Mechanics, vol VIIA. ISRM, Denver, pp 27–32
- Bieniawski ZT (1979) The geomechanics classification in rock engineering applications. Proceedings of the 4th ISRM Congress. International Society for Rock Mechanics, Montreux 2:41–48
- Bieniawski ZT (1989) Engineering rock mass classifications: a complete manual for engineers and geologists in mining, civil, and petroleum engineering. John Wiley & Sons, pp 5–272
- Bureau of Indian Standard (1998) (Reaffirmed 2002) IS: 8764 Method of determination of point load index of rocks. BIS, New Delhi, pp 1–9
- Cai M, Kaiser PK, Uno H, Tasaka Y, Minami M (2004) Estimation of rock mass deformation and strength of jointed hard rock masses using GSI system. *Int J Rock Mech Min Sci* 41:3–19
- Cai M, Kaiser PK, Tasaka Y, Minami M (2007) Determination of residual strength parameters of jointed rock masses using the GSI system. *Int J Rock Mech Min Sci* 44(2):247–265
- Chen Z (1995) Recent developments in slope stability analysis. Proceedings of the 8<sup>th</sup> International Congress of Rock Mechanic (Fujii T, ed) 3:1041–1049
- Deere DU (1963) Technical description of rock cores for engineering purposes. *Felsmechanik Ingenieurgeologie* 1:16–22
- Dixit A, Pal AK, Jana A, Sreedeeep S (2017) Effect of geological strength index on factor of safety of jointed rock slope. Proceeding of Indian Geotechnical Conference IIT Guwahati, India, pp 1–3
- Geological Survey of India (GSI) (1999) Geological quadrangle map of Himachal Pradesh. Mineral resources of Himachal Pradesh, p 32
- Hoek E, Brown ET (1997) Practical estimates of rock mass strength. *Int J Rock Mech Min Sci* 34(8):1165–1186
- Hoek E, Marinos PG (2000) Predicting tunnel squeezing problems in weak heterogeneous rock masses. *Tunn Tunn Int* 132(11):45–51
- Hoek E, Brown ET (2019) The Hoek-Brown failure criterion and GSI e 2018 edition. *J Rock Mech Geotech Eng* 11(3):445–463
- Hoek E, Kaiser PK, Bawden WF (1995) Support of underground excavations in hard rock Rotterdam: A.A. Balkema, pp 58–65
- Hoek E, Marinos P, Benissi M (1998) Applicability of the geological strength index (GSI) classification for very weak and sheared rock masses. The case of the Athens schist formation. *Bull Eng Geol Environ* 57(2):151–160
- Hoek E, Carter TG, Diederichs MS (2013) Quantification of geological strength index chart. American Rock Mechanics Association (ARMA 13-672), 47<sup>th</sup> US Rock Mechanics-Geomechanics Symposium, San Francisco, pp 1–8
- Janardhana MR, Abdul-Aleam A, Al-Qadhi AD (2018) Slope stability assessment in and around Taiz city, Yemen using Landslide Possibility Index (LPI). *Eur J Adv Eng Technol* 5(1):8–17
- Khan AU, Prasad S (1996) Geological quadrangle map of Himachal Pradesh and Uttar Pradesh. Ed Director Map Project-III. Map and Cartography Division, GSI-NR Geological Survey of India, Kolkata, pp 45–66
- Marinos V (2017) A revised geotechnical classification GSI system for tectonically disturbed rock masses, such as flysch. *Bull Eng Geol Environ* 19:1e14. <https://doi.org/10.1007/s10064-017-1151-z>
- Marinos V, Carter TG (2018) Maintaining geological reality in application of GSI for design of engineering structures in rock. *Eng Geol* 239:282–297
- Marinos V, Marinos P, Hoek E (2005) The geological strength index: applications and limitations. *Bull Eng Geol Environ* 64:55–65
- Palmstrom A (2005) Measurements of and correlations between block size and rock quality designation (RQD). *Tunn Undergr Space Technol* 20:362–377
- Rocscience (2019) [www.rocscience.com-2D](http://www.rocscience.com-2D) and 3D Geotechnical software
- Romana M (1985) New adjustment ratings for application of Bieniawski classification to slopes. *Proc Int Symp Role Rock Mech*:49–53
- Romana (1993) A geomechanical classification for slopes: slope mass rating. *Rock Test Site Charact*:575–600. <https://doi.org/10.1016/B978-0-08-042066-0.50029-X>
- Prihutama FA, Fahmi B (2018) Geological strength index and rock mass rating for slope stability analysis, case study: geoheritage site pillow lava, Berbah, Yogyakarta. *AIP Conf Proc* 1987:020072 (2018). <https://doi.org/10.1063/1.5047357>
- Salmanfarsi AF, Awang H, Ali MI (2020) Rock mass classification for rock slope stability assessment in Malaysia a review. *IOP Conf. Series Materials Science and Engineering* 712, pp 1-9
- Singh B, Goel RK (1999) Rock mass classification—a practical approach in Civil Engineering. Elsevier, Amsterdam, pp 12–267
- Sonmez H, Ulusay R (2002) A discussion on the Hoek-Brown failure criterion and suggested modifications to the criterion verified by slope stability case studies. *Yerbilimleri* 26:77–99
- Taheri A (2012) Design of rock slopes using SSR classification system. International Conference on Ground Improvement and Ground Control, Wollongong, Australia, pp 12–18
- Taheri A, Tani K (2007) Rock slope design using slope stability rating (SSR) – Application and field verification. in Proc of 1st Canada-U.S. Rock Mechanics Symposium, pp 215–221



- Taheri A, Taheri A, and Tani K (2006) A modified rock mass classification system for preliminary design of rock slopes. in Proc. of 4<sup>th</sup> Asian Rock Mechanics Symposium, pp 1–8
- Tomás R, Delgado J, Serón JB (2007) Modification of slope mass rating (SMR) by continuous functions. *Int J Rock Mech Min Sci* 44:1062–1069
- Wyllie DC, Mah CW (2004) *Rock slope engineering: civil and mining*, 4th edn, pp 10–120
- Zheng J, Zhao Y, Lü Q, Deng J, Pan X, Li Y (2016) A discussion on the adjustment parameters of the slope mass rating (SMR) system for rock slopes. *Eng Geol* 206:42–49